HHS Public Access

Author manuscript

Adv Funct Mater. Author manuscript; available in PMC 2017 June 14.

Published in final edited form as:

Adv Funct Mater. 2016 June 14; 26(22): 3818–3836. doi:10.1002/adfm.201504185.

Magnetic Nanoparticle Facilitated Drug Delivery for Cancer Therapy with Targeted and Image-Guided Approaches

Dr. Jing Huang,
Department of Radiology and Imaging Sciences, Emory University School of Medicine, Atlanta, GA 30322, USA

Dr. Yuancheng Li,
Department of Radiology and Imaging Sciences, Emory University School of Medicine, Atlanta, GA 30322, USA

Dr. Anamaria Orza,
Department of Radiology and Imaging Sciences, Emory University School of Medicine, Atlanta, GA 30322, USA

Dr. Qiong Lu,
Department of Pharmacy, The Second Xiangya Hospital of Central South University, Changsha, Hunan 410011, China

Dr. Peng Guo,
Department of Biomedical Engineering, The City College of New York, New York, NY 10031, USA. Vascular Biology Program, Boston Children's Hospital, Boston, MA 02115, USA

Dr. Liya Wang,
Department of Radiology and Imaging Sciences, Emory University School of Medicine, Atlanta, GA 30322, USA

Prof. Lily Yang, and
Department of Surgery, Emory University School of Medicine, Atlanta, GA 30322, USA

Prof. Hui Mao
Department of Radiology and Imaging Sciences, Emory University School of Medicine, Atlanta, GA 30322, USA

Lily Yang: lyang02@emory.edu; Hui Mao: hmao@emory.edu

Abstract

With rapid advances in nanomedicine, magnetic nanoparticles (MNPs) have emerged as a promising theranostic tool in biomedical applications, including diagnostic imaging, drug delivery and novel therapeutics. Significant preclinical and clinical research has explored their functionalization, targeted delivery, controllable drug release and image-guided capabilities. To further develop MNPs for theranostic applications and clinical translation in the future, we attempt to provide an overview of the recent advances in the development and application of MNPs for drug delivery, specifically focusing on the topics concerning the importance of biomarker targeting

Correspondence to: Lily Yang, lyang02@emory.edu; Hui Mao, hmao@emory.edu.

for personalized therapy and the unique magnetic and contrast-enhancing properties of theranostic MNPs that enable image-guided delivery. The common strategies and considerations to produce theranostic MNPs and incorporate payload drugs into MNP carriers are described. The notable examples are presented to demonstrate the advantages of MNPs in specific targeting and delivering under image guidance. Furthermore, current understanding of delivery mechanisms and challenges to achieve efficient therapeutic efficacy or diagnostic capability using MNP-based nanomedicine are discussed.

1. Introduction

Actual therapeutic effect on diseased tissues, with negligible systemic toxicity toward normal organs or tissues, is dependent on the effective delivery of therapeutics to the diseased sites, which cannot be realized by most of the conventional therapeutics alone. Generally, intravenously (i.v.) administered drugs with low molecular weights are cleared out of the body rapidly even before they accumulate in the diseased tissue. In addition, the off-targeting distribution of conventional drugs within the body results in unwanted side effects where cytotoxic drugs are internalized by normal cells as well as by the primary target, such as a tumor.[1,2] This is a specific challenge in cancer chemotherapy utilizing potent drugs that are highly toxic to both cancerous and normal cells. Recent advances in nanomedicine have shown promise for targeted delivery of personalized treatment with natural and engineered nanomaterials. Compared with traditional medicine, nanomedicine has shown unique advantages in improving drug delivery and treatment efficacy, including: (i) passive or active targeting to the diseased tissue, (ii) prolonged drug circulation time without being cleared from the body rapidly, (iii) improved solubility of drugs, (iv) effective protection of payload therapeutic agents from inactivation or biodegradation, (v) controlled or sustained release of drugs, (vi) reduced systemic toxicity of highly potent but toxic drugs, and (vii) multifunctional and multimodal treatments through simultaneous delivery of multiple therapeutic agents to overcome drug resistance. Up to now, several nanoparticle based drug formulations have been approved by United States Food and Drug Administration (U.S. FDA) for cancer treatment, such as, Abraxane,[3] Doxil,[4] and Onivyde. Currently, more than 80 newly developed therapeutic nano-formulations are under investigation in preclinical studies and clinical trials. In spite of the great potential demonstrated by nanomedicine, future development and translation of efficient delivery of nanotherapeutics are needed to overcome several major challenges in order to make a real impact on clinical care of patients. In particular, there is a need in new strategies for improving efficiency with localized precision delivery and quantitative assessment of drug delivery and treatment response.

Magnetic nanoparticles (MNPs) composited with metallic, alloyed metallic, ferrites (MFe_2O_4, M = Fe, Co, Ni, Mn) and magnetic elements doped ferrites have been widely investigated as drug delivery systems. The advantages of MNPs, as illustrated in Figure 1, are built upon their availability and unique physical/chemical properties, such as simple and robust preparation methods, good biocompatibility, reactive functional groups on the surface, and magnetic responsiveness. The most widely studied and applied MNPs are iron oxide nanoparticles (IONPs), or superparamagnetic iron oxide nanoparticles (SPIOs) as

referred in some other literatures, due to their well-known excellent biocompatibility compared with other heavy metal containing nanomaterials (e.g., quantum dots, gold nanoparticles, or carbon nanotubes (CNTs)) that are hard to be degraded and eliminated from the body.[5] Five IONPs (Gastromark, Feridex, Resovist, Sinerem, and Ferumoxytol) have been approved by the U.S. FDA and/or the European Commission (EC) as magnetic resonance imaging (MRI) contrast agents (Gastromark, Feridex, Resovist, and Sinerem) or iron supplement for treating iron deficiency (Ferumoxytol). These approved IONPs are made mostly through co-precipitation method without any functionalization, and found accumulating mainly in the liver and spleen (50–80%), in which IONPs are then ingested and converted into the form suitable for iron storage.[7,8] Clinical doses of IONPs in humans are determined between 0.56–3 mg Fe/kg patient body weight, which is much less than the normal blood iron concentration (≈33 mg Fe/kg body weight) and relatively low compared with total body iron (≈3,500 mg). Although the potential toxicity is determined by particle component, size, shape, surface charge, coating materials, etc., a variety of MNPs have shown no significant or minimal negative effect on the liver or kidney function after i.v. administration.[7,8] Following functionalization with targeting ligands and drugs, increased amount of MNPs may accumulate at the targeted site via passive or active targeting to improve the therapeutic efficacy and even allowing a more aggressive/higher drug dosage. In addition, unique magnetic properties of MNPs enable MRI for evaluation of drug delivery efficiency, image guidance during delivery process, non-invasive monitoring of treatment responses, and external magnetic stimulated manipulations, such as magnetic field guided localization and hyperthermia, to enhance delivery and/or combined therapeutic effect. Hence, MNPs are excellent candidates for targeted drug delivery and image-guided therapeutics that have the potential for novel clinical applications in individualized medicine.

In this review, we provide an overview of recent advances in the development and applications of MNPs for drug delivery with a focus on the strategies of targeted and image-guided drug delivery. Several topics in this area are discussed, including MNP carrier fabrications, delivery mechanisms, active targeting approaches, and image-guided drug deliveries. Finally, concluding remarks and future perspectives for MNP drug delivery are presented.

2. Magnetic Nanoparticles as Drug Carriers

The design and preparation of functionalized MNPs for drug delivery require interdisciplinary approaches, taking into consideration of the physico-chemical properties of materials (i.e., payload drugs and drug carriers), their behaviors and responses in the biological or physiological environment, and the intended functions that address relevant medical problems. In order to have efficient drug delivery, MNP-based drug carriers should be able to: (i) possess the capacity of loading sufficient drug molecules, (ii) protect drug bioactivity and enhance biocompatibility, (iii) target to the intended delivery sites with less uptake by the normal organs and/or tissue. Depending on the needs of a given size uniformity and crystallinity of MNPs or simplicity of the preparation methods, a number of preparation methods have been developed and adopted to produce the core of MNPs with uniform size, controlled shape, and desirable compositions, including co-precipitation,[7] thermal decomposition,[8] hydrothermal deposition,[9] direct reduction,[10]

microemulsion,[11] and polyol synthesis[12], etc. Using MNPs as core materials, various functional organic (e.g., polymer,[13] lipid,[14] and protein[15]) or inorganic (e.g., gold,[16] silica,[17–19] graphene oxide,[20] and CNTs[21]) materials can be assembled with MNPs to provide the capacity of incorporating payload drugs to improve drug solubility for the systemic delivery.

Surface modification is usually required to make MNPs compatible with the properties of therapeutic agents, so that the drugs can be properly loaded and effectively released after delivering to the diseased sites. The most commonly used drug loading methods include direct encapsulation or adsorption of the drugs through physical interactions (e.g., hydrophobic interaction or electrostatic attraction) between the MNPs and the drug molecules or chemical reactions (e.g., covalent bonding through active groups) between the surface functional groups of MNPs and drug molecules, as shown in Figure 2. Drug loading efficiency can be highly dependent on the structures and polarities of drugs, the compositions and capacity of coating materials used in MNPs, and the numbers of functional groups on MNP surfaces. Therefore, engineering MNPs with appropriate coating materials and controlled surface properties is a common strategy to improve the drug loading. It has been shown that more hydrophobic drugs can be encapsulated into the coating layer of MNPs (e.g., 15 wt% of DOX loading) by increasing the thickness or porousness of the hydrophobic layer of the amphiphilic polymer coating.[22] In some cases, additional coating layers (e.g., polyethylene glycol (PEG) and protein) are applied to further protect payload drugs from premature release, and to conjugate targeting moieties via covalent bonding through specific crosslinkers (e.g., EDC/NHS, SPDP, and SMCC) or click chemistry (i.e., azide group) as illustrated in Figure 2. Table 1 summarizes some therapeutic agents that have been investigated as payload drugs for MNP-based delivery and several related methods used for drug loading and releasing.

2.1. Drug Loading through Hydrophobic Interactions

Hydrophobic therapeutic agents (e.g., doxorubicin, camptothecin, paclitaxel, etc.) that consist of more than 40% of currently used chemotherapy agents, are poorly soluble in the aqueous physiological conditions, resulting in very limited delivery efficacy.[23] However, those hydrophobic drugs can be easily incorporated into the hydrophobic layer of amphiphilic polymers that are commonly used to stabilize MNPs, driven by their hydrophobic interaction between each other and the repulsion from aqueous surroundings as illustrated in Figure 3A.[22,24,25] In a typical process, a hydrophobic drug is first dissolved into an organic solvent with appropriate polarity (e.g., DMSO, DMF, and methanol), followed by soaking the engineered MNPs in drug solution, in which the polymer coating may swell, allowing the drug diffuse to the hydrophobic coating layer/cavities. Subsequent products are collected and re-dispersed into the aqueous solution, resulting in the collapse of the inner hydrophobic layers beneath the hydrophilic outer layers. Hydrophobic drugs can be well preserved in the hydrophobic layers during the delivery process, and then released slowly after long time exposure to the physiological conditions or relatively fast under specific conditions. Such a sustained release profile is essential to maintaining a sufficient level of nanoparticle-drug carriers in the circulation, in order to deliver into the diseased tissues subsequently, which cannot be achieved by small molecule drugs that are cleared

rapidly. Once accumulated in the targeted site, encapsulated hydrophobic drugs can be released through different mechanisms. Change of the polarity of drug molecules or tissue/cellular environment may lead to the release of encapsulated drug molecules. For example, with pH-responsive polymer coatings (e.g., mPEG-b-poly(methacrylic acid)-b-poly(glycerol monomethacryate) and mPEG-poly(L-asparagine)), drugs can be released after MNPs arrived at lower-pH sites, such as tumor interstitial (pH 6.5–6.8) or cellular endosome/lysosome (pH 4.5–5.5), stemming from the protonation of the coating polymers that change structure or hydrophilicity,[26] or the dissociation of coating layer from the MNP core.[27] Since MNPs are able to induce a hyperthermia effect under an alternating magnetic field (AMF), thermo-responsive triggering is another mechanism to release the drugs that loaded in MNP carriers through hydrophobic interaction. During the exposure to AMF, MNPs may generate heat that increases temperature to a few degrees higher than the phase transition temperature (T_g) of the thermosensitive polymers, leading to the softening and swelling of the polymer phase, and subsequent release of loaded drugs. For example, Hayashi et al. used thermosensitive amphiphilic polymer (polymerized pyrrole-3-carboxylic acid (PyCOOH)) coated MNPs to load Dox, and observed more than 60% of the Dox content was released at T_g (≈44 °C), and about 90% at 46 °C when exposed to an AMF (230 kHz, 8 kA m^{-1}.[28] The remote, on-demand release of anticancer drugs assisted by AMF largely enhances the specificity of drug delivery as the temperature and direction can be easily regulated by using AMF.

2.2. Drug Loading through Covalent Bonds

Conjugating or cross-linking therapeutic agents to the functional groups on the functionalized MNP surface is another approach to carry payload drugs. The covalent bonding of drug molecules to the surface of MNPs is stable enough to secure drug molecules remaining on the MNP carriers during in vivo delivery. However, the release of pay-load drugs is relatively difficult. Therefore, a cleavable linkage between drugs and MNPs is usually used to enable the selective and controlled release of the drug molecules. The most commonly used cleavable linkers include amide and hydrazone bonds, which can be cleaved under lysosomal pH (pH = 5.0) to release the loaded drugs (e.g., Dox, methotrexate, paclitaxel, etc.)[29,30] Besides the pH-responsive bonds, given a specific enzyme-cleavable linker, the release of pay-load drugs can be highly controlled. For example, Lee et al. developed theranostic MNPs with chemotherapy agent gemcitabine (Gem) conjugated on the surface of IONPs via a cleavable tetrapeptide linker that can be cleaved by the enzyme cathepsin B, a protease located in the lysosome of cells (Figure 3B).[31] After the receptor-mediated endocytosis of the ATF-IONP-Gem into pancreatic tumor cells, Gem was then released intracellularly in the lysosomes upon the cleavage of the peptide linker by cathepsin B. The intracellular release is critical as Gem is much more potent and efficient in killing pancreatic cancer cells given its action of blocking DNA replication.

In addition, thermal induced linker cleavage has also been explored when using MNPs as drug carriers. For example, after conjugating with the surface coating that composed of a dextran-based polymer through hydrazone bond, Dox can be released from MNP carriers by a phase transition at the lower critical solution temperature of 38 °C.[32] N'Guyen et al. showed that magnetically induced hyperthermia could provide sufficient local energy to

trigger the retro-Diels-Alder process, thus breaking a linkage formed by a “click” reaction.[33] Notably, “click” reactions and other bioorthogonal reactions are widely used for the targeting ligand conjugation but rarely for drug loading due to the stability of the formed chemical bonds.[34]

Several issues have to be considered when using covalent bonding to load/carry drugs. First, the limited number of active functional groups on the surface of MNPs may restrict the drug loading amount. Secondly, this approach requires proper criteria or design of the linker and reactions with strictly controlled reaction conditions. Furthermore, the bioactivity of the loaded drugs, as well as the MNP stability, may be affected during the chemical reactions.

2.3. Drug Loading through Electrostatic Interactions

Electrostatic interactions are typically used for loading of nucleic acid and nucleotide drugs for gene therapy. For DNA or small interfering RNA (siRNA), cationic coating polymers, such as PEI,[36,37] polyamidoamine,[38] or chitosan[39] are employed as coating materials to interact with the negatively charged nucleic acids. These coating materials not only protect the nucleic acids from enzymatic degradation, but also facilitate the endosomal release of nucleic acids through “proton sponge effect”,[40] in which massive accumulation of protons is induced in endosomes leading to its osmotic swelling and consequently the burst release of nucleic acids into the cytoplasm.[41] In general, in vivo applications of these systems are limited due to the toxicity and stability concerns.[2] However, a recent study has demonstrated that PEI-PEG-Chitosan copolymer coated MNPs and MNP–polymer composite interlayer with a relatively neutral lipid shell can be utilized as a safe carrier for gene delivery both in vitro and in vivo (Figure 3C).[35,42]

2.4. Drug Loading through Direct Encapsulation

Liposomes and micelles that are composed of amphiphilic molecules can be used for direct encapsulation of MNPs and therapeutic agents. Both of them exhibit remarkable capability in accommodating both hydrophilic[43] and hydrophobic MNPs.[44] For example, using an amphiphilic biodegradable poly(lactic-*co*-glycolic acid) polymer, MNPs and quantum dots can be encapsulated together with the anticancer drug busulfan,[45] where a 32% of degradation of the micelle into lactic and glycolic acid over five weeks was observed in the in vitro study. By combining gold nanoparticle as radiosensitizer and MNPs as MRI contrast agents into micelles as shown in Figure 3D, image-guided radiotherapy was demonstrated to be effective in a human fibrosarcoma xenograft tumor mouse model (Figure 3D).[46] Another example is Amstad et al. embedded small MNPs that are stabilized with palmitylnitroDOPA into the lipid membranes but not the cavities to better control the drug release.[47] Upon the stimulation of AMF, MNPs in the liposome bilayers generated heat to increase local temperature to the membrane melting temperature (T_m, 55 °C), which is much higher than the bulk temperature, to release the drug without disrupting the liposome structure. Besides liposomes and micelles, other materials (e.g., zeolite and mesoporous silica) have also been employed for drug encapsulation. MNPs and small molecules, including fluorescein and an anticancer drug camptothecin, could be encapsulated in the zeolitic imidazolate framework-8 (ZIF-8), forming a drug loaded nanocomposite of 70 nm sized that can dissociate in the endosome to release the cargo.[48]

3. Targeted Delivery of Theranostic MNPs

3.1. EPR Driven Passive Targeting

The delivery of theranostic nanoparticles, such as MNPs, to the diseased tissues, particular in cancer treatment, is initially driven by the enhanced permeability and retention (EPR) effect. The EPR effect, first reported by Maeda and his colleagues in 1986,[49,50] describes the enhanced permeability of the tumor vasculature that allows macromolecules, lipids, and nanoparticles circulating in the blood to extravasate through the leaky tumor blood vessel, then enter the tumor interstitial space.[51] Meanwhile, dysfunctional or lack of lymphatic drainage in tumor further retains the MNPs within the tumor by preventing nanoparticles getting back to the circulation.[50,52] As a result systemically administered nanoparticles can preferentially accumulate in tumor tissues, leading to passive targeting of a tumor without targeting ligands. In contrast to normal tissues and organs, most solid tumors feature rapidly developed tumor vasculature with loose tight-junction and fenestration of endothelial cells, and abnormal or missing basement membrane of blood vessels, which collectively cause increased tumor vasculature permeability.[49,53,54] Fenestrations presented in the tumor blood vessel walls have a size range of 200 to 2000 nm,[54,55] allowing MNPs to pass through the leaky vessel walls.

To take advantage of the EPR effect mediated passive targeting of the tumor, the size of drug-MNP assembly needs to be smaller than the fenestrations in tumor vessel walls (200–2000 nm) for extravasations. Once extravasated, the penetration of the drug carrying MNPs into the tumor tissues is a diffusion-mediated process, which is inversely correlated with the particle size. Thus, considerable research has been focused on finding the optimized particle size for EPR-mediated delivery.[56–58] In general, MNPs with sizes in the range of 10–500 nm are believed to be suited for EPR effect-mediated tumor accumulation.[56] On the other hand, surface charge of theranostic MNPs also plays an important role in EPR-mediated passive tumor targeting. It has been shown that the luminal surface of vascular endothelial layer is negatively charged, therefore, nanoparticles with the cationic charge can rapidly interact with endothelial cells, causing non-specific binding that shortens the plasma half-life, and a consequently reduced the EPR effect.[59] Nanoparticles with highly negative charges are prone to be trapped by organs in the reticuloendothelial system (RES) such as liver and spleen. However, MNPs with neutral surface charge are difficult to be sterically stabilized. Taking together, a slightly negative surface charge of MNPs is considered to be better for a longer blood circulation time, though the surface charge is not a dominant factor for blood clearance, which is more dependent on MNP size and component.[60] Besides the size and surface charge, the shape of MNPs is another critical factor regulating the MNP drug delivery. It has been known that nanomaterials with elongated structures and shape demonstrate favorable pharmacokinetic and tumor-homing properties compared to their spherical counterparts.[61] This is because nanomaterials with high aspect ratios have a larger surface area than spherical particles, offering more potential binding sites for functionalization, and consequently greater loading with targeting ligands, imaging agents and/or drugs. Steinmetz et al. reported that the rod-like, high aspect ratio, viral nanovector showed enhanced tumor homing and tissue penetration properties than the spherical viral nanovectors.[61]

3.2. Ligand Facilitated Active Targeting

While passive targeting through the EPR effect provides the general mechanism for delivering a broad range of nanoparticle carriers, targeting ligand facilitated active targeting of molecular or cellular biomarkers further enhances the precision and targeted delivery of the therapeutic agents that are biomarker specific and require direct interactions of the drug molecules and biomarkers. Furthermore, active targeting with binding of the ligand conjugated MNPs to over expressed cell surface receptors promotes the intracellular delivery of therapeutic agents through receptor mediated endocytosis, as shown in Figure 4. For example, transferrin (Tf, 80 kDa) is an iron-chelating protein that targets transferrin receptor (TfR, 180 kDa, also known as CD71), a transmembrane glycoprotein.[62,63] Generally the overexpression of TfR can be observed on the surfaces of proliferating cancer cells due to an increased iron requirements but its level in many normal tissues is low. TfR-mediated Tf internalization is a very fast process (less than 5 min), leading to the turnover rate of 20,000 Tf/cell/min.[64] This allows greater accumulation of Tf conjugated MNPs at the target site, resulting in a stronger contrast and higher local drug concentration.[65] In addition, the consistent TfR expression level through all tumor development stages makes TfR a more reliable biomarker for tumor targeting and drug delivery.[64]

Typically targeting ligands can be categorized into proteins, peptides, aptamers, and small molecules. Antibodies and other functional proteins are natural choices of targeting ligands because of their high specificity and affinity toward the disease biomarkers. Furthermore, some antibodies carry the therapeutic effect by themselves. For example, Herceptin (commercially marketed as Trastuzumab) is monoclonal antibody used to treat early stage (curable) breast cancer with high expression of HER2/neu receptor which is a human epidermal growth factor receptor essential for cell proliferation. Trastuzumab treatment improved overall survival and disease-free survival of HER2-positive breast cancer patients. Herceptin can be also used as the ligand for targeting HER2-positive breast cancer.[67] Hence, Herceptin conjugated MNPs have been developed for HER2-positive breast cancer imaging and treatment.[67–69]

Given the concerns of immunogenic side effect, stability and the high cost usually associated with antibody production for translational and clinical applications, antibody fragment or synthetic peptides with well-preserved structures and functions of the binding domain to the target can be prepared as targeting ligands. Single-chain anti-EGFR antibody (ScFvEGFR) is an antibody fragment with molecular weight ranging from 25 to 28 kDa and less than 20% of the whole antibody, yet maintains the high binding affinity and specificity toward EGFR.[70] The ScFvEGFR conjugated IONPs have been investigated for targeted cancer imaging and therapy.[71,72] Urokinase-type plasminogen activator receptor (uPAR) is a multidomain glycoprotein attached to the cell membrane. It has an elevated expression level in many human cancers.[73] uPAR becomes an attractive biomarker in cancer because of its critical roles in cell migration, proliferation, and survival by coordinating extracellular matrix (ECM) proteolysis and cell signaling.[73] Urokinase plasminogen activator (uPA) is the natural ligand with a high affinity for uPAR. The amino-terminal fragment (ATF) of uPA has been successfully utilized to conjugate MNPs for uPAR targeting in breast cancer,[74–76] pancreatic cancer,[31,76] and prostate cancer.[77] Recently, near infrared dye NIR-830 labeled

insulin-like growth factor 1 (IGF-1) was used as a targeting ligand to conjugate with IONP for targeted delivery of Dox into IGF-1R positive pancreatic cancer in a orthotopic human pancreatic cancer patient tissue derived xenograft model (PDX) in nude mice. Targeted delivery of IGF-1-IONPs loaded with Dox into pancreatic tumors following systemic administration of the nanoparticles was demonstrated by T_2-weighted MRI (Figure 5).[22]

Another noteworthy class of targeting ligand is aptamers, which are synthetic single-stranded oligonucleotides that are capable of binding specific targets with high affinity.[78] Aptamers are synthesized through successive rounds of in vitro selection, purification, and amplification to yield oligo-nucleotides with high affinity for a specific antigen.[79] More recent techniques allow in vitro selection to be carried out with whole living cells to create aptamers for specific cell lines.[80] By combining MNPs with the excellent recognition capability of aptamers, aptamers conjugated MNPs have shown increased binding affinity for the target through a multivalent binding effect.[81] With a variety of aptamers being developed, the aptamer-MNP system has been tested for targeted imaging/therapy in prostate cancer,[82,83] and colorectal cancer.[84]

Some low molecular weight small molecules can also be used as targeting moieties if they demonstrate sufficient affinity to the targets. The folate receptor (FR) is a glycosyl-phosphatidylinositol-linked membrane protein expressed on the cell surface. The FR is typically overexpressed in cancerous tissues[62] but expressed in limited quantities on the surface of normal epithelial cells of kidney, thyroid, lung, and brain.[85] It has been reported that folic acid (FA) conjugated SPIOs demonstrated 3- to 16-fold higher uptake in FR-expressing cancer cells compared to non-conjugated SPIOs.[86] In vivo study also exhibited decreased signal intensity and enhanced contrast in tumor MRI after the injection of FA conjugated SPIOs.[87] Methotrexate (MTX) is a small molecule analogue of folic acid that can target the overexpressed folate receptors on the cancer cell surface.[88] MTX conjugated MNPs have been studied for targeted MR imaging and drug delivery of glioma.[30] Given that MTX is also a therapeutic agent, the MTX functions not only as a ligand for tumor targeting, but also as a drug when released after breaking the MTX-MNP linkage by lysosome. Integrins are transmembrane glycoproteins that are involved in the communication between cells and the extracellular matrix (ECM).[89] Among the 24 known integrins, $\alpha_v\beta_3$ is of particular interest as cancer biomarker and target for in vivo diagnostics and therapeutics, because of its key role in tumor angiogenesis as well as the high expression levels on tumor cells of various origin.[90] Arginylglycylaspartic acid, also called RGD peptide, is a tripeptide composed of L-arginine, glycine, and L-aspartic acid that can specifically bind with integrin $\alpha_v\beta_3$ overexpressed on cancer cells. RGD peptide has been widely used as a nanoparticle targeting ligand to facilitate tumor specific molecular imaging and drug delivery.[91–93] For instance, Luo et al. have reported the application of RGD conjugated ultrasmall MNPs (2.7 nm in diameter) in T_1-weighted MRI of gliomas in mice.[91] Meanwhile, the cyclic RGD is preferred over the linear form to be conjugated onto MNPs, due to the greater affinity to integrin $\alpha_v\beta_3$ and better stability.[92]

3.3. Surface Functionalization with Targeting Ligands

Targeting ligands can be attached to the surface of MNPs via covalent bonding and non-covalent bonding. Albeit ligand conjugation with MNPs via non-covalent binding is relatively easier to operate, several pitfalls, such as reproducibility, stability in biological media, etc., limit its wide applications.[94] On the other hand, the covalent conjugation of targeting ligands is normally adopted for MNP surface functionalizations, and a number of methods have been developed. Generally the active groups on the MNP surface for ligand conjugation include amine, carboxyl, hydroxyl, and aldehyde. By using these active groups, ligands can be conjugated either directly to the MNPs or through one of the cross-linkers summarized in Table 2.

For direct conjugation of ligands, MNP surface is typically functionalized with amine (-NH_2) groups or carboxyl (-COOH) groups. Coupling reaction between amine and carboxyl is widely used in the conjugation of MNPs with a variety of ligands, such as aptamers,[82] proteins,[95] and small molecules,[96] for in vivo targeted MRI and drug delivery. Anhydrides are typically used in small molecule ligand conjugation by forming stable covalent bonds with amine groups.[96] When conjugating with carboxyl (-COOH) group on the surface of MNPs, amine groups from proteins, peptides, and aptamers are directly coupled by forming amide bonds with the assistance of coupling reagents, i.e., 1-ethyl-3-(3-dimethylaminopropyl)-carbodiimide (EDC) and *N*-hydroxysuccinimide (NHS). The MNP-conjugates are extensively investigated in vivo for tumor imaging and therapy in breast cancer,[74] prostate cancer,[75–77,97] and pancreatic cancer.[22,31,71,76] Additionally, aldehyde (-CHO) group can also be used for ligand conjugation on the MNP surfaces. Aldehyde group is well-known to react with primary amine to form Schiff base.[98,99] However, the formation of Schiff base is a reversible process. In order to establish stable covalent bonds between aldehyde-bearing MNPs and protein/monoclonal antibodies, a reducing agent has to be added to convert unstable -C=N- to stable -C-N-.[84,100].

Given the limited functional groups available for direct ligand conjugation with MNPs, various linker molecules have been developed to accomplish the conjugation that cannot be achieved by direct coupling. Amine groups on the surface of MNPs can be activated with *N*-succinimidyl iodacetate (SIA) to be ready for reaction with thiol groups. After peptides are thiolated, they can be facilely conjugated to the MNPs. This method has been used for in vivo imaging of gliomas,[101] and pancreatic cancer.[102] Amine groups can also be activated by attaching maleimide molecules, which is highly specific for coupling with thiols through thiolene ‘click’ chemistry. This conjugation has been reported for in vivo glioma targeting.[103] ‘Click’ reaction between alkyne and azide has been reported for ligand conjugation with MNPs. The amine groups are modified with synthetic linker to provide azide groups on the surface of MNPs. Peptides functionalized with alkynes are conjugated afterwards. This approach has been documented for in vivo tumor targeting.[104] Sulfosuccinimidyl 6-[3′(2-pyridyldithio)-propionamido] hexanoate (Sulfo-LC-SPDP) can be utilized in the coupling between amine groups on MNPs and amines on antibodies/peptides. Once the amine groups (both on MNPs and ligands) are activated by Sulfo-LC-SPDP, the SPDP moieties form a disulfide bond to make the MNPs functionalized with targeting ligands.[69] When thiol groups present on the MNP surface for functionalization, the amine

groups on monoclonal antibodies can be activated by sulfosuccinimidyl 4-(*N*-maleimidomethyl)cyclohexane-1-carboxylate (sulfo-SMCC) to introduce maleimide groups. The stable and highly specific coupling between thiol and maleimide makes this approach suitable for in vivo MRI of tumors.[105]Although rarely used for ligand conjugation, hydroxyl groups can react with epichlorohydrin and 2,2′-(ethylenedioxy) bisethylamie (EDBE) to introduce amine groups for conjugation. Carboxyl groups from proteins can be covalently conjugated to the MNPs, and the resulting MNP conjugate has been investigated in breast cancer imaging in vivo.[68]

4. Strategies to Enhance Targeted Delivery of MNP Carriers

4.1. Tuning the Size and Shape of MNPs for Enhanced EPR effect

As we mentioned in Section 3.1, the EPR effect occurs in a size-dependent manner, and MNPs with sizes in the range of 10–500 nm are believed to be better for EPR effect-mediated tumor accumulation in general.[56] However, novel strategies have been reported recently to further improve the accumulation of MNPs in tumors. For example, Jain and his co-workers showed reducing the sizes of fenestrations in the walls of vessels through the anti-angiogenesis treatment, a procedure named “tumor vasculature normalization”, significantly decreased the interstitial fluid pressure in tumors and demonstrated a more rapid nanoparticle (size <12 nm) extravasation.[57] On the other hand, tumor vasculature normalization increased steric and hydrodynamic hindrances, and make it more difficult for large nanoparticles (size >12 nm) to enter tumors. Thus, Jain’s results suggested that small nanoparticles (size ≈12 nm) are ideal for tumor vasculature normalization-mediated drug delivery. Ling et al. reported on the fabrication of tumor pH-sensitive magnetic nanogrenades (termed PMNs) composed of self-assembled 3 nm IONPs and pH-responsive ligands. These PMNs can readily target tumors via surface-charge switching triggered by the acidic tumor microenvironment, and are further disassembled into highly active state in acidic subcellular compartments that “turns on” MRI contrast, fluorescence, and photodynamic therapeutic activity, as shown in Figure 6.[106] Although high aspect ratio MNPs showed enhanced tumor penetration,[119] developing MNPs with a high aspect ratio is still challenging. However, this can be achieved by advanced synthetic chemistry and self-assembly nanotechnology. Peiris et al. reported that chain-like MNPs made of multiple spherical magnetic IONPs (about 20 nm core sizes) covalently linked to each other through a single bond can efficiently penetrate the blood brain barrier (BBB) and preferentially accumulate in glioblastoma multiforme (GBM) tumors after docking on the endothelia layer of the tumor blood vasculature through active targeting of tumor vasculature through conjugated RGD ligands interacting with tumor specific $\alpha_v\beta_3$ integrin. When coupling the MNP chain with a liposome loaded with Dox, which does not cross BBB alone, this nanochain carrier was able to deliver 4.7% of administered dose into GBM tumors, 2.7-fold more drugs than the spherical shaped MNPs, resulting in a 18.6-fold greater drug dose administered to brain tumors than standard chemotherapy.[107]

4.2. Reducing Non-Specific Uptake and Prolonging Retention Time

Surface modification of MNPs has a direct impact on its blood clearance, and consequently has an important influence on the EPR effect, ligand-to-target affinity and drug release.

When applied systemically through vascular delivery, nanoparticles are subject to immediate interactions with blood, a complex biological medium with high ionic strength and various proteins and cells.[108] Plasma proteins will non-specifically adsorb onto the surface of nanoparticles, also known as opsonization, forming a stable protein layer called corona. The presence of the protein corona is responsible for the fast clearance of nanoparticles by the mononuclear phagocyte system (MPS), particularly macrophages,[109] and the reticuloendothelial system (RES), such as the liver, spleen, and lung.[110] The opsonization and non-specific cellular uptake of nanoparticles result in the substantial reduction in targeting efficiency and the off-target distribution of nanoparticles as well as unwanted cytotoxicity from the drug loaded on nanoparticles. Protein corona also changes the drug release profile of nanocarriers.[94] Conventionally, dextran or PEG coating provides MNP a more hydrophilic surface that can reduce plasma protein adsorption via hydrophilicity and steric repulsion effects with the consequently prolonged circulation time in blood stream [111] long enough to reach and extravasate the leaky tumor vasculature, eventually improving the EPR effect.[112] For example, Doxil, a clinically approved, PEGylated liposomal anti-cancer drug, demonstrated a significantly longer circulation half-life of 55 h than those of Myocet, Doxil's non-PEGylated counterpart (2.5 h), and the free form of Doxorubicin (0.2 h).[113] PEGylation is currently the most widely used technique for MNP coating. After the MNP coated with PEG (PEGylated), the reduction of non-specific cellular uptake of MNPs has been reported.[60] More recently, new coating polymers with anti-biofouling property and better performance on the reduction of non-specific cellular uptake and elongation of blood circulating time are developed.[108,114] These copolymers typically contain hydrophobic moieties to anchor on the surface of MNPs. It has been reported that the hydrophobic layer provide protection to the coating materials from being replaced by biomolecules.[115] The factors determining the anti-biofouling property are still under investigation. It is believed to related to the length of PEG, the terminal functional groups on PEG, and the density of PEG distribution on the surface of nanoparticles.[116] Zwitterionic polymers are significant complements to PEG on anti-biofouling coating materials. Electroneutral materials are believed to be more effective in reducing non-specific interactions with biological system.[2,94] Opposite to PEG, which contains no charge, zwitterionic polymers bear both positive and negative charges on the same polymer molecule. The non-charged moiety attaches to the surface of MNPs through anchoring group, while the charged moiety will fold because of the electrostatic interactions, resulting in a protective "shield" around the MNPs. The zwitterionic polymers were initially developed to inhibit the adhesion of protein and bacteria and the formation of biofilm.[117] Recent in vivo investigations using zwitterionic polymer coated MNPs have shown comparable anti-biofouling effect to PEG-based coating materials.[118]

4.3. Magnetic Field Enhanced Local Delivery and Controlled Release

Since MNPs are highly responsive to an external magnetic field, such very unique property makes it possible to apply magnetic field directed targeting and local delivery of the MNP drug carriers. By positioning an external magnet or gradient magnetic field in the diseased site, drug carrying MNPs may navigate through the physiological medium and locally accumulated in the area driven by the magnetic force from the locally applied field. In this case, MNPs with high magnetic susceptibility likely possess higher local delivery efficiency.

Magnetic targeting has been demonstrated highly effective for in vitro drug delivery compared with other targeting ligand mediated delivery.[37] However, limited by the non-adjustable attractive strength and the short active reach-out range, external magnetic field or force based magnetic targeting is only suitable for the diseased area that are fairly superficial or therapy that may need a minimal invasive procedure.[119,120] In recent years, gradient magnetic field has been proved to be a useful tool to direct MNP carriers. For example, Muthana et al. utilized the magnetic field gradient coil in a 7 T MRI scanner to demonstrate image-guided magnetic resonance targeting delivery of stimulated macrophages in an orthotopic prostate cancer mouse model.[121] With the magnetic targeting, the macrophage viral therapy (human monocyte-derived macrophages (MDMs) carried oncolytic virus HSV1716) exhibited greater inhibition on tumor growth and metastasis.

Under an alternating magnetic field (AMF), MNPs generate heat through Neel and Brownian relaxation, together with the hysteresis loss.[122] This magnetocaloric effect is utilized to heat up the diseased tissues accumulated with MNPs to reach a temperature that is high enough (>40 °C) to enhance the reactivity and stimulate the drug release. By modifying temperature responsive materials, MNP drug carriers can control the drug release by applying external AMF. The heat generated by MNP changes the structure of the surrounding temperature sensitive materials that usually turns into loose swollen structures, leading to the release of loaded drugs.[13,17] MNPs can also serve as sealing materials for those drug storage vehicles (e.g., mesoporous silica).[18] A controllable switching of those drug storage pools can be realized by the guidance of magnetic field according to the demands.

5. MNPs-Based Image-Guided Delivery and Therapy

5.1. Visualizing Drug Delivery in vivo with MNPs

MNPs enable MRI-guided drug delivery, thereby offering the advantage of imaging tools to visualize drug distribution, assess targeted delivery efficiency, and monitor/trigger drug release/therapeutic process. Efforts have been made in optimizing MNPs based nanocarriers, together with proper imaging technologies. Currently, most MNP based image-guided drug delivery relies on, but not limited to, the MRI signal changes resulting from MNP induced MRI contrast changes, mostly by shortening T_1 and T_2 relaxation times or perturbation in susceptibility. Such MNP induced contrast enhancement enables the direct visualization of MNP drug delivery systems in tissues, including small molecule drugs,[22,25,31] siRNA,[123] proteins,[124] and labeled cells[125]. Hadjipannayis et al. employed IONPs to carry the epidermal growth factor receptor variant III (EGFRvIII) antibody to the U87ΔEGFRvIII mouse xenograft model of human glioblastoma multiforme (GBM) tumor.[124] Successful delivery of EGFRvIII into tumors and subsequently slow dispersion of MNP carriers at the tumor sites were evidenced by in vivo T_2-weighted MRI on days 4 and 7 after MNPs were administered. This treatment resulted in a significant increase in animal survival. However, the negative T_2- or T_2*-weighted MRI are known to have drawbacks in differentiating the areas of interest from the artifacts and poor contrast when background tissues have low signal, such as the tumors located in the peritoneal cavity. Recently, an ultrashort TE (UTE) MRI based on T_1 or a positive contrast enhancement from MNPs was introduced to visualize

the MNP labeled cells and MNPs administered to animals.[126] T_1-weighted UTE MRI was demonstrated to enhance the detecting sensitivity of residual pancreatic tumors in the peritoneal cavity of mice bearing orthotopic human pancreatic tumor after the treatment with IONPs conjugated with uPAR targeting ATF ligand and chemotherapy agent gemcitabine (ATF-IONP-Gem) for targeted delivery of Gem to pancreatic cancerous and stromal cells (Figure 7A). ATF-IONP-Gem accumulation in the tumor was captured by bright T_1 contrast from IONPs in tumors with UTE imaging.[31] as well as signal drops in T_2-weighted MRI, demonstrating higher tumor accumulation of ATF-IONP-Gem than non-targeted IONP-Gem and thus provided a more efficient tumor inhibition effect. Although largely under development, the strategies for quantifying drug delivery using MNPs have been explored based on the relationships between MRI signal changes and MNP concentration,[127] a potential critical capability for MNP based image-guided drug delivery system. Mouli et al. directly compared the efficiency of different drug delivery strategies with IONPs loaded with Dox by quantitatively measuring the ΔR_2^* of the tumors (Figure 7B).[128] Combination therapy of nanoablation and nanoembolization was found to be the most efficient way to deliver Dox loaded MNPs into the tumor, with the greatest T_2^* signal drop in both the tumor core and periphery areas. Ex vivo ICP-MS quantification of the tumors further confirmed the greatest uptake of Dox loaded MNPs in the combination therapy.

Besides visualizing and quantifying the delivery location and amount, MNPs can also provide longitudinal information about the drug status (i.e., released or not). Generally, MRI contrast agents (normally Gd chelate agents) are incorporated with drugs in liposomes or polymer based micelles. Non-invasive MRI can monitor the delivery and quantify the released contents via the contrast changes. Rizzitelli et al. detected the release of Dox from nanocarriers that incorporated Dox with MRI contrast agent Gadoteridol in liposome.[129] A significant increase in T_1 contrast to noise ratio (CNR) in tumors was observed after pLINFU stimulation, indicating the successful release of Gadoteridol and Dox from the liposome. The drug concentration can be monitored by this CNR (T_1), which showed a spike after stimulation, and decreased within 6 h, following slow increase from day 1 to day 3 and 4 and then diminished on day 7. Li et al. also reported T_1 MR signal enhancement in the periphery area of the tumor at 60 min after i.v. injection of their nanoplex, composed of PEI/siRNA-chk/PLL-DOTA-Gd/Cy5.5/bCD-111, and in the central region of the tumor after 24 h and 48 h.[130] siRNA-mediated down-regulation of Chk-α and the conversion of 5-FC to 5-FU by the prodrug enzyme bacterial cytosine deaminase (bCD) were monitored noninvasively with ^{1}H MR spectroscopic imaging and ^{19}F MR spectroscopy (Figure 8). The spatio-temporal guidance of the drug release provided by MRI allowed for evaluating the therapeutic efficiency individually to assure the on-time adjustment of the treatment plan.

Other imaging approaches, such as ultrasound,[108] photoacoustic,[99,120,131–133] CT,[134] PET/SPECT,[135] and optical[22,25,133–135] imaging, have been involved in the MNPs-based image-guided drug delivery, in order to provide more accurate image guidance. Multimodal imaging approaches can be readily achieved by combining MNPs with other imaging moieties. Recently we developed an oral drug delivery system based on milk protein coated IONP, in which model drug ICG was incorporated into the inner polymer layer.[25] The successful delivery of MNPs with protein coating protection to the small intestine was observed by both MRI and NIR imaging, while the bare MNPs without protein coating was

observed being trapped in the stomach. Another example by Zhou et al. demonstrated systemic delivery of IGF1 conjugated IONP carrying Dox with MRI assessment of the drug delivery in a human pancreatic cancer PDX model, showing higher delivery efficiency and therapeutic effect of targeted IGF1-IONP-Dox.[22] Using ^{125}I labeled fluorescent silica coated IONPs (^{125}I-fSiO4@SPIOs), Tang et al. quantitatively tracked labeled mesenchymal stem cells (MSC) transplanted intracerebrally or intravenously into stroke rats by MRI/SPECT/fluorescent trimodal imaging.[135] The signal lasted up to 14 days, allowing for the determination of MSCs distribution after both groups showed improved neurobehavior. IC-injected MSCs was found to migrate to the lesion site along the corpus callosum, while IV-injected MSCs were mainly trapped in lung.

5.2. Image-Guided Combination Therapy with MNPs

In addition to visualizing drug delivery with MRI or multimodal imaging, MNPs advance in combination therapy with image-guided deposition of exogenous energy. Either MNPs or the loaded nanoresponsors are stimulated to generate high temperature or trigger drug release via light,[131] magnetic,[107] acoustic[129] or radioactive energy.[46] Among them, hyperthermia has been considered as an additive therapy method of chemotherapy and radiotherapy, where high temperature (>40 °C) that accelerates cell apoptosis is achieved by applying AMF at the diseased sites that accumulated with MNPs.[122] For example, improved in vivo therapeutic efficacy was observed for the combination of hyperthermia and chemotherapy of multiple myeloma by using smart MNP carriers loaded with Dox (Figure 9).[28] Although magnetic hyperthermia produced by radiofrequency/AMF emerged as the earliest approach, the discomfort at higher magnetic field strengths and irregular intratumoural heat distribution limit its application.[136] The ongoing research mainly focuses on developing more efficient MNPs to escape from RES uptake and effectively target to the lesions. The combination of magnetic hyperthermia and radiotherapy has been proved to be clinically effective in brain cancer and prostate cancer patients undergoing phase II trials in humans.[137] Other researches have tried to enhance the therapeutic effect by combining MNPs with radiosensitive materials/drugs (e.g., gold nanoparticles and Mitomycin C).[46,138]

Recently, photothermal therapy under MRI guidance has attracted great attention because of its convenience and effi-cacy. Photo-absorbing nanomaterials, such as upconversion materials,[139] metal sulfide nanoparticles (e.g., Co_9Se_8[131] and FeS[140]), carboneous materials (e.g., graphene oxide,[141] Fe_2C_5,[99] porphyrin[132] and polypyrrole[142]), NIR dyes (e.g., IR825[133] and Pheophorbide A[143]), and gold nanomaterials[144] are integrated with MNPs to generate heat at the desired location indicated by MRI anatomic information, and being monitored with the temperature by MR thermometry (e.g., proton resonance frequency shift method).

High intensity focused ultrasound (HIFU) is considered to be another promising hyperthermia methodology that elevates MNPs-based drug delivery. This approach delivers high-frequency focused mechanical sound waves through an ultrasound transducer to generate heat locally in the tissue.[145] During the process, the temperature-sensitive liposomes loaded with drug and MRI contrast agents are disrupted to provide MR contrast in

real time.[13] The changes of local tissue pressure and possible tissue displacement induced by acoustic energy may facilitate the permeation and diffusion of the released drugs into deep tissue and target cells. [146]

6. Conclusion and Perspectives

With increased emphasis on precision medicine, the targeted and image-guided drug delivery is expected to play a major role in the individualized treatment of human cancers and other diseases. Highly heterogeneous human cancer cells and tumor microenvironment requires novel drug delivery approaches and non-invasive imaging methods to assess drug delivery efficiency and tumor responses to the therapy in individual patients. Although genomic profiling of tumor biopsy tissues, a common approach for precision medicine, may characterize the disease based on intrinsic properties of tumor cells that may be associated with drug sensitivity, it is difficult to provide the information on the efficiency of drug delivery to tumors in individual patients at different stages of tumor development and under a particular treatment or different treatments since tumor vasculatures and tumor microenvironment affect intratumoral drug delivery and distribution. MNP-based drug carriers have great potentials to deliver precision oncology with assistance of imaging capabilities, such as MRI, therefore, offering non-invasive and longitudinal imaging assessment to evaluate biomarker targeted nanoparticle-drug delivery and even intratumoral distribution of the drug carrier, because determining the option for biomarker targeted treatment and the need of targeted therapy delivery as well as treatment monitoring may be a part of the very early step in the treatment planning in the practice of precision medicine. Additionally, multifunctional MNPs enable delivery of combination drugs, stimulation controlled drug release, sensitizing drug action that can lead to improved therapeutic sensitivity. It is expected that engineered MNPs continue to be an attractive platform for the future development of theranostic applications that implement the targeted and image-guided delivery. The future development of MNPs for drug delivery applications are dependent on the more and better understanding of the nanoparticle delivery mechanisms in various diseases. The systematical investigation and new knowledge on the interface between the engineered nanomaterials and biological environments at various physical conditions, anatomic locations and different tissue environments are necessary when designing and implementing MNPs based drug delivery systems to a specific biological system or disease. Developing innovative ideas and approaches to explore potential functions and capabilities of MNPs in drug delivery and imaging applications should have clear vision on the healthcare problems and clinical applications. While a wide range of engineered MNPs are developed for drug delivery in laboratory research and preclinical studies, the clinical translations of these developed new nanomaterials are challenging. There are urgent needs in addressing several issues in translational research. Optimized and scale-up ready MNP fabrications are essential to developing pre-clinical and clinical applications. Standardization of MNP characterizations with quantitative assessments of their efficacies and capabilities is of critical importance and needs to be established. To improve the clearance and safety and significantly decrease the off-target effects of theranostic MNPs in normal organs, such as liver and spleen, current research efforts have focused on the development of a new generation of ultrafine MNPs (<3 nm) with high

biodegradability for fast clearance[147] and anti-fouling polymer coating for reducing nonspecific uptake by macrophages and RES organs. As nanomedicine continues to grow and makes impact on future medicine, there is a promising future for a broad range of clinical applications of MNP-based image-guided targeted delivery.

Acknowledgments

This work is supported in parts by NIH R01CA154846-04 (HM and LY), NCI's Cancer Nanotechnology Platform Project (CNPP) grant (U01CA151810-05 to HM and LY), Children's Healthcare of Atlanta Center for Pediatric Nanomedicine Seed Grant (HM). Authors thank Ms. Donna Kilcullen for her editorial assistance and proofreading of the manuscript.

References

1. a) Dobson J. Drug Dev Res. 2006; 67:55.b) Sun C, Lee JSH, Zhang M. Adv Drug Delivery Rev. 2008; 60:1252.
2. Veiseh O, Gunn JW, Zhang M. Adv Drug Delivery Rev. 2010; 62:284.
3. Green MR. Ann Oncol. 2006; 17:1263. [PubMed: 16740598]
4. Barenholz Y. J Controlled Release. 2012; 160:117.
5. Longmire M, Choyke PL, Kobayashi H. Nanomedicine. 2008; 3:703. [PubMed: 18817471]
6. Gu L, Fang RH, Sailor MJ, Park J-H. ACS Nano. 2012; 6:4947. [PubMed: 22646927]
7. Kang YS, Risbud S, Rabolt JF, Stroeve P. Chem Mater. 1996; 8:2209.
8. a) Park SJ, Kim S, Lee S, Khim ZG, Char K, Hyeon T. J Am Chem Soc. 2000; 122:8581.b) Park J, An K, Hwang Y, Park JG, Noh HJ, Kim JY, Park JH, Hwang NM, Hyeon T. Nat Mater. 2004; 3:891. [PubMed: 15568032]
9. Daou TJ, Pourroy G, Begin-Colin S, Greneche JM, Ulhaq-Bouillet C, Legare P, Bernhardt P, Leuvrey C, Rogez G. Chem Mater. 2006; 18:4399.
10. Hadjipanayis CG, Bonder MJ, Balakrishnan S, Wang X, Mao H, Hadjipanayis GC. Small. 2008; 4:1925. [PubMed: 18752211]
11. Santra S, Tapec R, Theodoropoulou N, Dobson J, Hebard A, Tan WH. Langmuir. 2001; 17:2900.
12. Wan J, Cai W, Meng X, Liu E. Chem Commun. 2007:5004.
13. Sanson C, Diou O, Thévenot J, Ibarboure E, Soum A, Brulet A, Miraux S, Thiaudière E, Tan S, Brisson A. ACS Nano. 2011; 5:1122. [PubMed: 21218795]
14. Plassat V, Wilhelm C, Marsaud V, Menager C, Gazeau F, Renoir J-M, Lesieur S. Adv Funct Mater. 2011; 21:83.
15. Huang J, Wang L, Lin R, Wang AY, Yang L, Kuang M, Qian W, Mao H. Acs Appl Mater Interfaces. 2013; 5:4632. [PubMed: 23633522]
16. Lee SM, Kim HJ, Ha YJ, Park YN, Lee SK, Park YB, Yoo KH. ACS Nano. 2012; 7:50. [PubMed: 23194301]
17. Thomas CR, Ferris DP, Lee JH, Choi E, Cho MH, Kim ES, Stoddart JF, Shin JS, Cheon J, Zink JI. J Am Chem Soc. 2010; 132:10623. [PubMed: 20681678]
18. Ruiz-Hernandez E, Baeza A, Vallet-Regi M. ACS Nano. 2011; 5:1259. [PubMed: 21250653]
19. Zhang L, Wang T, Yang L, Liu C, Wang C, Liu H, Wang YA, Su Z. Chem Eur J. 2012; 18:12512. [PubMed: 22907903]
20. Feng L, Li K, Shi X, Gao M, Liu J, Liu Z. Adv Healthcare Mater. 2014; 3:1261.
21. Fadel TR, Sharp FA, Vudattu N, Ragheb R, Garyu J, Kim D, Hong E, Li N, Haller GL, Pfefferle LD, Justesen S, Herold KC, Fahmy TM. Nat Nanotechnol. 2014; 9:639. [PubMed: 25086604]
22. Zhou H, Qian W, Uckun FM, Wang L, Yang YA, Chen H, Kooby D, Yu Q, Lipowska M, Staley CA, Mao H, Yang L. ACS Nano. 2015; 9:7976. [PubMed: 26242412]
23. Lipinski CA. J Pharmacol Toxicol Methods. 2000; 44:235. [PubMed: 11274893]
24. Chen Y-C, Lee W-F, Tsai H-H, Hsieh W-Y. J Biomed Mater Res Part A. 2012; 100A:1279.

25. Huang J, Shu Q, Wang L, Wu H, Wang AY, Mao H. Biomaterials. 2015; 39:105. [PubMed: 25477177]
26. a) Guo M, Yan Y, Zhang H, Yan H, Cao Y, Liu K, Wan S, Huang J, Yue W. J Mater Chem. 2008; 18:5104.b) Yu S, Wu G, Gu X, Wang J, Wang Y, Gao H, Ma J. Colloids Surf, B. 2013; 103:15.
27. Jain TK, Richey J, Strand M, Leslie-Pelecky DL, Flask C, Labhasetwar V. Biomaterials. 2008; 29:4012. [PubMed: 18649936]
28. Hayashi K, Nakamura M, Miki H, Ozaki S, Abe M, Matsumoto T, Sakamoto W, Yogo T, Ishimura K. Theranostics. 2014; 4:834. [PubMed: 24955144]
29. a) Chang Y, Meng X, Zhao Y, Li K, Zhao B, Zhu M, Li Y, Chen X, Wang J. J Colloid Interface Sci. 2011; 363:403. [PubMed: 21821262] b) Liu D, Wu W, Chen X, Wen S, Zhang X, Ding Q, Teng G, Gu N. Nanoscale. 2012; 4:2306. [PubMed: 22362270]
30. Kohler N, Sun C, Fichtenholtz A, Gunn J, Fang C, Zhang M. Small. 2006; 2:785. [PubMed: 17193123]
31. Lee GY, Qian WP, Wang L, Wang YA, Staley CA, Satpathy M, Nie S, Mao H, Yang L. ACS Nano. 2013; 7:2078. [PubMed: 23402593]
32. Zhang J, Misra RDK. Acta Biomater. 2007; 3:838. [PubMed: 17638599]
33. N'Guyen TTT, Duong HTT, Basuki J, Montembault V, Pascual S, Guibert C, Fresnais J, Boyer C, Whittaker MR, Davis TP, Fontaine L. Angew Chem Int Ed. 2013; 52:14152.
34. Tassa C, Shaw SY, Weissleder R. Acc Chem Res. 2011; 44:842. [PubMed: 21661727]
35. Hu S-H, Hsieh T-Y, Chiang C-S, Chen P-J, Chen Y-Y, Chiu T-L, Chen S-Y. Adv Healthcare Mater. 2014; 3:273.
36. Chertok B, David AE, Yang VC. Biomaterials. 2010; 31:6317. [PubMed: 20494439]
37. Rao, Y-f; Chen, W.; Liang, X-g; Huang, Y-z; Miao, J.; Liu, L.; Lou, Y.; Zhang, X-g; Wang, B.; Tang, R-k; Chen, Z.; Lu, X-y. Small. 2015:11.
38. Pan B, Cui D, Sheng Y, Ozkan C, Gao F, He R, Li Q, Xu P, Huang T. Cancer Res. 2007; 67:8156. [PubMed: 17804728]
39. Bhattarai SR, Kim SY, Jang KY, Lee KC, Yi HK, Lee DY, Kim HY, Hwang PH. J Virol Methods. 2008; 147:213. [PubMed: 17935796]
40. a) McBain SC, Griesenbach U, Xenariou S, Keramane A, Batich CD, Alton EW, Dobson J. Nanotechnology. 2008; 19:405102. [PubMed: 21832609] b) Mykhaylyk O, Zelphati O, Rosenecker J, Plank C. Curr Opin Mol Ther. 2008; 10:493. [PubMed: 18830925]
41. Huth S, Lausier J, Gersting SW, Rudolph C, Plank C, Welsch U, Rosenecker J. J Gene Med. 2004; 6:923. [PubMed: 15293351]
42. Kievit FM, Veiseh O, Bhattarai N, Fang C, Gunn JW, Lee D, Ellenbogen RG, Olson JM, Zhang M. Adv Func Mater. 2010; 19:2244.
43. Martina M-S, Fortin J-P, Menager C, Clement O, Barratt G, Grabielle-Madelmont C, Gazeau F, Cabuil V, Lesieur S. J Am Chem Soc. 2005; 127:10676. [PubMed: 16045355]
44. Frascione D, Diwoky C, Almer G, Opriessnig P, Vonach C, Gradauer K, Leitinger G, Mangge H, Stollberger R, Prassl R. Int J Nanomed. 2012; 7:2349.
45. Ye F, Barrefelt A, Asem H, Abedi-Valugerdi M, El-Serafi I, Saghafian M, Abu-Salah K, Alrokayan S, Muhammed M, Hassan M. Biomaterials. 2014; 35:3885. [PubMed: 24495486]
46. McQuade C, Al Zaki A, Desai Y, Vido M, Sakhuja T, Cheng Z, Hickey RJ, Joh D, Park S-J, Kao G, Dorsey JF, Tsourkas A. Small. 2015; 11:834. [PubMed: 25264301]
47. Amstad E, Kohlbrecher J, Müller E, Schweizer T, Textor M, Reimhult E. Nano Lett. 2011; 11:1664. [PubMed: 21351741]
48. Zhuang J, Kuo C-H, Chou L-Y, Liu D-Y, Weerapana E, Tsung C-K. ACS Nano. 2014; 8:2812. [PubMed: 24506773]
49. Maeda H, Nakamura H, Fang J. Adv Drug Delivery Rev. 2013; 65:71.
50. Matsumura Y, Maeda H. Cancer Res. 1986; 46:6387. [PubMed: 2946403]
51. a) Iyer AK, Khaled G, Fang J, Maeda H. Drug Discovery Today. 2006; 11:812. [PubMed: 16935749] b) Fang J, Nakamura H, Maeda H. Adv Drug Delivery Rev. 2011; 63:136.c) Nichols JW, Bae YH. J Controlled Release. 2014; 190:451.

52. a) Iwai K, Maeda H, Konno T. Cancer Res. 1984; 44:2115. [PubMed: 6324996] b) Konno T, Maeda H, Iwai K, Maki S, Tashiro S, Uchida M, Miyauchi Y. Cancer. 1984; 54:2367. [PubMed: 6093980]
53. Folkman J. N Engl J Med. 1971; 285:1182. [PubMed: 4938153]
54. Hashizume H, Baluk P, Morikawa S, McLean JW, Thurston G, Roberge S, Jain RK, McDonald DM. Am J Pathol. 2000; 156:1363. [PubMed: 10751361]
55. Hobbs SK, Monsky WL, Yuan F, Roberts WG, Griffith L, Torchilin VP, Jain RK. Proc Natl Acad Sci USA. 1998; 95:4607. [PubMed: 9539785]
56. Peer D, Karp JM, Hong S, Farokhzad OC, Margalit R, Langer R. Nat Nanotechnol. 2007; 2:751. [PubMed: 18654426]
57. Chauhan VP, Stylianopoulos T, Martin JD, Popović Z, Chen O, Kamoun WS, Bawendi MG, Fukumura D, Jain RK. Nat Nanotech. 2012; 7:383.
58. a) Maeda, H.; Greish, K.; Fang, J. Polymer Therapeutics II. Satchi-Fainaro, R.; Duncan, R., editors. Vol. 193. Springer-Verlag; Berlin/Heidelberg: 2006. p. 103b) Maeda H. Adv Enzyme Regul. 2001; 41:189. [PubMed: 11384745] c) Maeda H, Bharate GY, Daruwalla J. Eur J Pharm Biopharm. 2009; 71:409. [PubMed: 19070661] d) Maeda H. Adv Drug Delivery Rev. 2001; 46:169.
59. a) Gusev SA, Povalĭ TM, Volobueva TM, Zakharchenko VN. Tsitologiia. 1988; 30:1022. [PubMed: 3206542] b) Campbell RB, Fukumura D, Brown EB, Mazzola LM, Izumi Y, Jain RK, Torchilin VP, Munn LL. Cancer Res. 2002; 62:6831. [PubMed: 12460895]
60. Reddy LH, Arias JL, Nicolas J, Couvreur P. Chem Rev. 2012; 112:5818. [PubMed: 23043508]
61. Shukla S, Ablack AL, Wen AM, Lee KL, Lewis JD, Steinmetz NF. Mol Pharm. 2013; 10:33. [PubMed: 22731633]
62. Islam T, Josephson L. Cancer Biomarkers. 2009; 5:99. [PubMed: 19414927]
63. Daniels TR, Delgado T, Rodriguez JA, Helguera G, Penichet ML. Clin Immun. 2006; 121:144.
64. Kresse M, Wagner S, Pfefferer D, Lawaczeck R, Elste V, Semmler W. Magn Reson Med. 1998; 40:236. [PubMed: 9702705]
65. Rosen JE, Chan L, Shieh D-B, Gu FX. Nanomed: Nanotechnol Biol Med. 2012; 8:275.
66. Valsecchi ME, McDonald M, Brody JR, Hyslop T, Freydin B, Yeo CJ, Solomides C, Peiper SC, Witkiewicz AK. Cancer. 2012; 118:3484. [PubMed: 22086503]
67. Ross JS, Fletcher JA, Bloom KJ, Linette GP, Stec J, Symmans WF, Pusztai L, Hortobagyi GN. Mol Cell Proteomics. 2004; 3:379. [PubMed: 14762215]
68. Chen T-J, Cheng T-H, Chen C-Y, Hsu SCN, Cheng T-L, Liu G-C, Wang Y-M. J Biol Inorg Chem. 2009; 14:253. [PubMed: 18975017]
69. Chen H, Wang L, Yu Q, Qian W, Tiwari D, Yi H, Wang AY, Huang J, Yang L, Mao H. Int J Nanomed. 2013; 8:3781.
70. a) Zhou Y, Drummond DC, Zou H, Hayes ME, Adams GP, Kirpotin DB, Marks JD. J Mol Biol. 2007; 371:934. [PubMed: 17602702] b) Adams GP, Schier R. J Immunol Methods. 1999; 231:249. [PubMed: 10648942]
71. Yang L, Mao H, Wang YA, Cao Z, Peng X, Wang X, Duan H, Ni C, Yuan Q, Adams G, Smith MQ, Wood WC, Gao X, Nie S. Small. 2009; 5:235. [PubMed: 19089838]
72. Liang H, Li X, Chen B, Wang B, Zhao Y, Zhuang Y, Shen H, Zhang Z, Dai J. J Controlled Release. 2015; 209:101.
73. Smith HW, Marshall CJ. Nat Rev Mol Cell Biol. 2010; 11:23. [PubMed: 20027185]
74. Yang L, Cao Z, Sajja HK, Mao H, Wang L, Geng H, Xu H, Jiang T, Wood WC, Nie S, Wang YA. J Biomed Nanotech. 2008; 4:439. www.MaterialsViews.com.
75. Yang L, Sajja H, Cao Z, Wang AY, Smith MQ, Bender L, Mao H, Nie S, Wood WC. Cancer Res. 2009; 69:348S.
76. Yang L, Mao H, Cao Z, Wang YA, Peng X, Wang X, Sajja HK, Wang L, Duan H, Ni C, Staley CA, Wood WC, Gao X, Nie S. Gastroenterology. 2009; 136:1514. [PubMed: 19208341]
77. Abdalla MO, Karna P, Sajja HK, Mao H, Yates C, Turner T, Aneja R. J Controlled Release. 2011; 149:314.
78. Liu Q, Jin C, Wang Y, Fang X, Zhang X, Chen Z, Tan W. NPG Asia Mater. 2014; 6:e95.

79. Tuerk C, Gold L. Science. 1990; 249:505. [PubMed: 2200121]
80. Shangguan D, Li Y, Tang Z, Cao ZC, Chen HW, Mallikaratchy P, Sefah K, Yang CJ, Tan W. Proc Natl Acad Sci USA. 2006; 103:11838. [PubMed: 16873550]
81. McCarthy JR, Weissleder R. Adv Drug Delivery Rev. 2008; 60:1241.
82. a) Farokhzad OC, Jon S, Khademhosseini A, Tran TNT, LaVan DA, Langer R. Cancer Res. 2004; 64:7668. [PubMed: 15520166] b) Dhar S, Gu FX, Langer R, Farokhzad OC, Lippard SJ. Proc Natl Acad Sci USA. 2008; 105:17356. [PubMed: 18978032]
83. Lupold SE, Hicke BJ, Lin Y, Coffey DS. Cancer Res. 2002; 62:4029. [PubMed: 12124337]
84. Toma A, Otsuji E, Kuriu Y, Okamoto K, Ichikawa D, Hagiwara A, Ito H, Nishimura T, Yamagishi H. Brit J Cancer. 2005; 93:131. [PubMed: 15970924]
85. a) Sudimack J, Lee RJ. Adv Drug Delivery Rev. 2000; 41:147.b) Lu Y, Low PS. J Controlled Release. 2003; 91:17.
86. a) Sonvico F, Mornet S, Vasseur S, Dubernet C, Jaillard D, Degrouard J, Hoebeke J, Duguet E, Colombo P, Couvreur P. Bioconjugate Chem. 2005; 16:1181.b) Sun C, Sze R, Zhang M. J Biomed Mater Res Part A. 2006; 78A:550.c) Chen TJ, Cheng TH, Hung YC, Lin KT, Liu GC, Wang YM. J Biomed Mater Res Part A. 2008; 87A:165.
87. Li L, Gao F, Jiang W, Wu X, Cai Y, Tang J, Gao X, Gao F. Drug Deliv. 2015
88. Peng X-H, Qian X, Mao H, Wang AY, Chen Z, Nie S, Shin DM. Int J Nanomed. 2008; 3:311.
89. a) Hood JD, Cheresh DA. Nat Rev Cancer. 2002; 2:91. [PubMed: 12635172] b) Hynes RO. Cell. 2002; 110:673. [PubMed: 12297042]
90. Schottelius M, Laufer B, Kessler H, Wester H-J. Acc Chem Res. 2009; 42:969. [PubMed: 19489579]
91. Luo Y, Yang J, Yan Y, Li J, Shen M, Zhang G, Mignani S, Shi X. Nanoscale. 2015; 7:14538. [PubMed: 26260703]
92. Zhang C, Jugold M, Woenne EC, Lammers T, Morgenstern B, Mueller MM, Zentgraf H, Bock M, Eisenhut M, Semmler W, Kiessling F. Cancer Res. 2007; 67:1555. [PubMed: 17308094]
93. Yang X, Hong H, Grailer JJ, Rowland IJ, Javadi A, Hurley SA, Xiao Y, Yang Y, Zhang Y, Nickles RJ, Cai W, Steeber DA, Gong S. Biomaterials. 2011; 32:4151. [PubMed: 21367450]
94. Laurent S, Mahmoudi M. Int J Mol Epid and Gene. 2011; 2:367.
95. Guo P, Huang J, Wang L, Jia D, Yang J, Dillon DA, Zurakowski D, Mao H, Moses MA, Auguste DT. Proc Natl Acad Sci USA. 2014; 111:14710. [PubMed: 25267626]
96. Weissleder R, Kelly K, Sun EY, Shtatland T, Josephson L. Nat Biotechnol. 2005; 23:1418. [PubMed: 16244656]
97. Wang AZ, Bagalkot V, Vasilliou CC, Gu F, Alexis F, Zhang L, Shaikh M, Yuet K, Cima MJ, Langer R, Kantoff PW, Bander NH, Jon S, Farokhzad OC. ChemMedChem. 2008; 3:1311. [PubMed: 18613203]
98. a) Li Y, Lee TB, Wang T, Gamble AV, Gorden AEV. J Org Chem. 2012; 77:4628. [PubMed: 22563758] b) Li Y, Wu X, Lee TB, Isbell EK, Parish EJ, Gorden AEV. J Org Chem. 2010; 75:1807. [PubMed: 20141120]
99. Yu J, Yang C, Li J, Ding Y, Zhang L, Yousaf MZ, Lin J, Pang R, Wei L, Xu L, Sheng F, Li C, Li G, Zhao L, Hou Y. Adv Mater. 2014; 26:4114. [PubMed: 24677251]
100. Zhao M, Beauregard DA, Loizou L, Davletov B, Brindle KM. Nat Med. 2001; 7:1241. [PubMed: 11689890]
101. a) Veiseh O, Sun C, Gunn J, Kohler N, Gabikian P, Lee D, Bhattarai N, Ellenbogen R, Sze R, Hallahan A, Olson J, Zhang M. Nano Lett. 2005; 5:1003. [PubMed: 15943433] b) Sun C, Veiseh O, Gunn J, Fang C, Hansen S, Lee D, Sze R, Ellenbogen RG, Olson J, Zhang M. Small. 2008; 4:372. [PubMed: 18232053]
102. Montet X, Weissleder R, Josephson L. Bioconjugate Chem. 2006; 17:905.
103. Chen K, Xie J, Xu H, Behera D, Michalski M, Biswal S, Wang A, Chen X. Biomaterials. 2009; 30:6912. [PubMed: 19773081]
104. Maltzahn, Gv; Ren, Y.; Park, J-H.; Min, D-H.; Kotamraju, VR.; Jayakumar, J.; Fogal, V.; Sailor, MJ.; Ruoslahti, E.; Bhatia, SN. Bioconjugate Chem. 2008; 19:1570.

105. Huh Y-M, Jun Y-w, Song H-T, Kim S, Choi S-s, Lee J-H, Yoon S, Kim K-S, Shin J-S, Suh J-S, Cheon J. J Am Chem Soc. 2005; 127:12387. [PubMed: 16131220]
106. Ling D, Park W, Park S, Lu Y, Kim KS, Hackett MJ, Kim BH, Yim H, Jeon YS, Na K, Hyeon T. J Am Chem Soc. 2014; 136:5647. [PubMed: 24689550]
107. Peiris PM, Abramowski A, Mcginnity J, Doolittle E, Toy R, Gopalakrishnan R, Shah S, Bauer L, Ghaghada KB, Hoimes C, Brady-Kalnay SM, Basilion JP, Griswold MA, Karathanasis E. Cancer Res. 2015; 75:1356. [PubMed: 25627979]
108. Kempen PJ, Greasley S, Parker KA, Campbell JL, Chang H-Y, Jones JR, Sinclair R, Gambhir SS, Jokerst JV. Theranostics. 2015; 5:631. [PubMed: 25825602]
109. Nie S. Nanomedicine. 2010; 5:523. [PubMed: 20528447]
110. a) Deng ZJ, Liang M, Monteiro M, Toth I, Minchin RF. Nat Nanotechnol. 2011; 6:39. [PubMed: 21170037] b) Nel AE, Madler L, Velegol D, Xia T, Hoek EMV, Somasundaran P, Klaessig F, Castranova V, Thompson M. Nat Mater. 2009; 8:543. [PubMed: 19525947]
111. a) Yu M, Huang S, Yu KJ, Clyne AM. Int J Mol Sci. 2012; 13:5554. [PubMed: 22754315] b) Otsuka H, Nagasaki Y, Kataoka K. Adv Drug Delivery Rev. 2003; 55:403.
112. Alexis F, Pridgen E, Molnar LK, Farokhzad OC. Mol Pharm. 2008; 5:505. [PubMed: 18672949]
113. Yeh M-K, Chang Hsin-I, Cheng Ming-Yen. Int J Nanomedicine. 2011:49. [PubMed: 22275822]
114. a) Chen H, Wu X, Duan H, Wang YA, Wang L, Zhang M, Mao H. ACS Appl Mater Interfaces. 2009; 1:2134. [PubMed: 20161520] b) Chen H, Wang L, Yeh J, Wu X, Cao Z, Wang YA, Zhang M, Yang L, Mao H. Biomaterials. 2010; 31:5397. [PubMed: 20398933]
115. Larson TA, Joshi PP, Sokolov K. ACS Nano. 2012; 6:9182. [PubMed: 23009596]
116. Walkey CD, Olsen JB, Guo H, Emili A, Chan WCW. J Am Chem Soc. 2012; 134:2139. [PubMed: 22191645]
117. Chen S, Liu L, Jiang S. Langmuir. 2006; 22:2418. [PubMed: 16519431]
118. a) Shao Q, Jiang S. Adv Mater. 2015; 27:15. [PubMed: 25367090] b) Li A, Leuhmann HP, Sun G, Samarajeewa S, Zou J, Zhang S, Zhang F, Welch MJ, Liu Y, Wooley KL. ACS Nano. 2012; 6:8970. [PubMed: 23043240]
119. Wang L, An Y, Yuan C, Zhang H, Liang C, Ding F, Gao Q, Zhang D. Int J Nanomedicine. 2015; 10:2507. [PubMed: 25848268]
120. Li Z, Yin S, Cheng L, Yang K, Li Y, Liu Z. Adv Funct Mater. 2014; 24:2312.
121. Muthana M, Kennerley AJ, Hughes R, Fagnano E, Richardson J, Paul M, Murdoch C, Wright F, Payne C, Lythgoe MF, Farrow N, Dobson J, Conner J, Wild JM, Lewis C. Nat Commun. 2015; 8:8009.
122. Kumar CSSR, Mohammad F. Adv Drug Delivery Rev. 2011; 63:789.
123. a) Kumar M, Yigit M, Dai G, Moore A, Medarova Z. Cancer Res. 2010; 70:7553. [PubMed: 20702603] b) Cho YS, Lee GY, Sajja HK, Qian W, Cao Z, He W, Karna P, Chen X, Mao H, Wang YA, Yang L. Small. 2013; 9:1964. [PubMed: 23292656]
124. Hadjipanayis CG, Machaidze R, Kaluzova M, Wang L, Schuette AJ, Chen H, Wu X, Mao H. Cancer Res. 2010; 70:6303. [PubMed: 20647323]
125. Cho IK, Moran SP, Paudyal R, Piotrowska-Nitsche K, Cheng P-H, Zhang X, Mao H, Chan AWS. Theranostics. 2014; 4:972. [PubMed: 25161700]
126. a) Zhang L, Zhong X, Wang L, Chen H, Wang YA, Yeh J, Yang L, Mao H. J Magn Reson Imag. 2011; 33:194.b) Wang L, Zhong X, Qian W, Huang J, Cao Z, Yu Q, Lipowska M, Lin R, Wang A, Yang L, Mao H. J Magn Reson Imag. 2014; 40:1071.
127. Huang J, Zhong X, Wang L, Yang L, Mao H. Theranostics. 2012; 2:86. [PubMed: 22272222]
128. Mouli SK, Tyler P, McDevitt JL, Eifler AC, Guo Y, Nicolai J, Lewandowski RJ, Li W, Procissi D, Ryu RK, Wang YA, Salem R, Larson AC, Omary RA. ACS Nano. 2013; 7:7724. [PubMed: 23952712]
129. Rizzitelli S, Giustetto P, Cutrin JC, Castelli DD, Boffa C, Ruzza M, Menchise V, Molinari F, Aime S, Terreno E. J Controlled Release. 2015; 202:21.
130. Li C, Penet M-F, Wildes F, Takagi T, Chen Z, Winnard PT Jr, Artemov D, Bhujwalla ZM. ACS Nano. 2010; 4:6707. [PubMed: 20958072]

131. Song X-R, Wang X, Yu S-X, Cao J, Li S-H, Li J, Liu G, Yang H-H, Chen X. Adv Mater. 2015; 27:3285. [PubMed: 25885638]
132. Liang X, Li Y, Li X, Jing L, Deng Z, Yue X, Li C, Dai Z. Adv Func Mater. 2015; 25:1451.
133. Gong H, Dong Z, Liu Y, Yin S, Cheng L, Xi W, Xiang J, Liu K, Li Y, Liu Z. Adv Funct Mater. 2014; 24:6492.
134. Yang G, Gong H, Liu T, Sun X, Cheng L, Liu Z. Biomaterials. 2015; 60:62. [PubMed: 25985153]
135. Tang Y, Zhang C, Wang J, Lin X, Zhang L, Yang Y, Wang Y, Zhang Z, Bulte JWM, Yang G-Y. Adv Func Mater. 2015; 25:1024.
136. Salunkhe AB, Khot VM, Pawar SH. Curr Topics Med Chem. 2014; 14:572.
137. a) Maier-Hauff K, Ulrich F, Nestler D, Niehoff H, Wust P, Thiesen B, Orawa H, Budach V, Jordan A. J Neuro-Oncol. 2011; 103:317.b) Johannsen M, Thiesen B, Wust P, Jordan A. Int J Hyperthermia. 2010; 26:790. [PubMed: 20653418]
138. Fan W, Shen B, Bu W, Zheng X, He Q, Cui Z, Zhao K, Zhang S, Shi J. Chem Sci. 2015; 6:1747.
139. He F, Yang G, Yang P, Yu Y, Lv R, Li C, Dai Y, Gai S, Lin J. Adv Func Mater. 2015; 25:3966.
140. Yang K, Yang G, Chen L, Cheng L, Wang L, Ge C, Liu Z. Biomaterials. 2015; 38:1. [PubMed: 25457978]
141. Wang S, Zhang Q, Luo XF, Li J, He H, Yang F, Di Y, Jin C, Jiang XG, Shen S, Fu DL. Biomaterials. 2014; 35:9473. [PubMed: 25175596]
142. Song X, Gong H, Yin S, Cheng L, Wang C, Li Z, Li Y, Wang X, Liu G, Liu Z. Adv Func Mater. 2014; 24:1194.
143. Nafiujjaman M, Revuri V, Nurunnabi M, Cho KJ, Lee Y-k. Chem Commun. 2015; 51:5687.
144. Sotiriou GA, Starsich F, Dasargyri A, Wurnig MC, Krumeich F, Boss A, Leroux J-C, Pratsinis SE. Adv Func Mater. 2014; 24:2818.
145. Fan C-H, Ting C-Y, Lin H-J, Wang C-H, Liu H-L, Yen T-C, Yeh C-K. Biomaterials. 2013; 34:3706. [PubMed: 23433776]
146. Lammers T, Koczera P, Fokong S, Gremse F, Ehling J, Vogt M, Pich A, Storm G, van Zandvoort M, Kiessling F. Adv Func Mater. 2015; 25:36.
147. Huang J, Wang L, Zhong X, Li Y, Yang L, Mao H. J Mater Chem B. 2014; 2:5344.

Biographies

Jing Huang received her Ph.D. from the College of Chemical and Molecular Engineering of Peking University in 2010. During her doctorate study, she worked on developing novel MRI contrast agents for biomedical imaging applications. She joined Dr. Hui Mao's laboratory in the Department of Radiology and Imaging Sciences at Emory University in 2011 as a postdoctoral researcher, and her current research is focused on magnetic nanomaterials-based nanotheranostics for targeted cancer imaging and therapy.

Yuancheng Li received his B.S. (2006) in applied chemistry from Beijing Technology and Business University, and Ph.D. (2012) in organic chemistry from Auburn University. He joined Dr. Hui Mao's research group as a postdoctoral researcher in Department of Radiology and Imaging Sciences at Emory University in 2012. Dr. Li's research interests include the development of novel nanomaterials for in vitro diagnosis and in vivo molecular imaging and therapy, and the metabolite detection and quantification by nuclear magnetic resonance spectroscopy.

Hui Mao is currently the Professor in the Department of Radiology and Imaging Sciences at Emory University and adjunct Professor in the Emory-Georgia Tech Joint Department of Biomedical Engineering. Research in Dr. Mao's laboratory is focused on developing and utilizing imaging technologies, especially magnetic resonance methods, to address biological questions and solve medical problems with strong emphases on translational research and potential clinical applications to the clinical management of major diseases, such as cancer and neurodegenerative diseases.

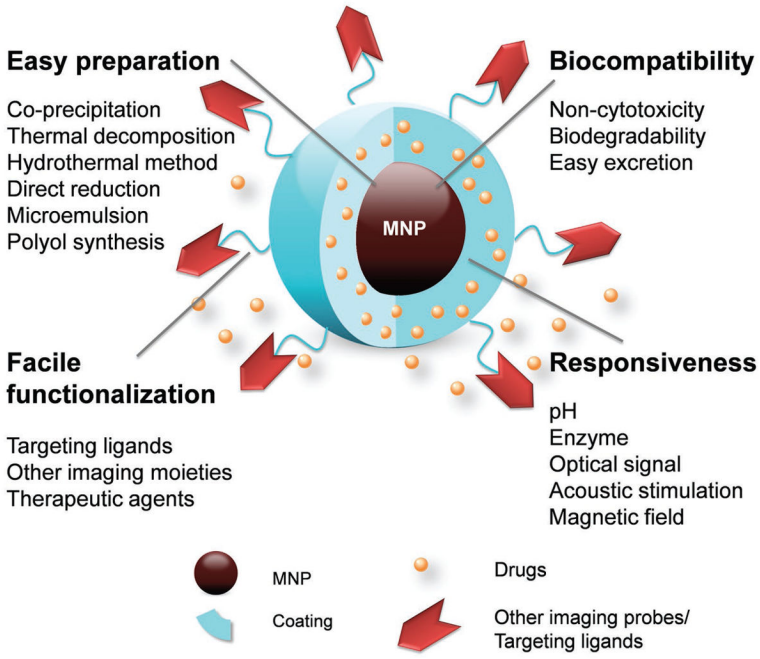

Figure 1.

Properties of MNPs for the development of drug delivery systems, including simple and robust preparation methods, good biocompatibility, facile functionalization through reactive functional groups on surface, and responsiveness to exogenous energy or specific physiological conditions.

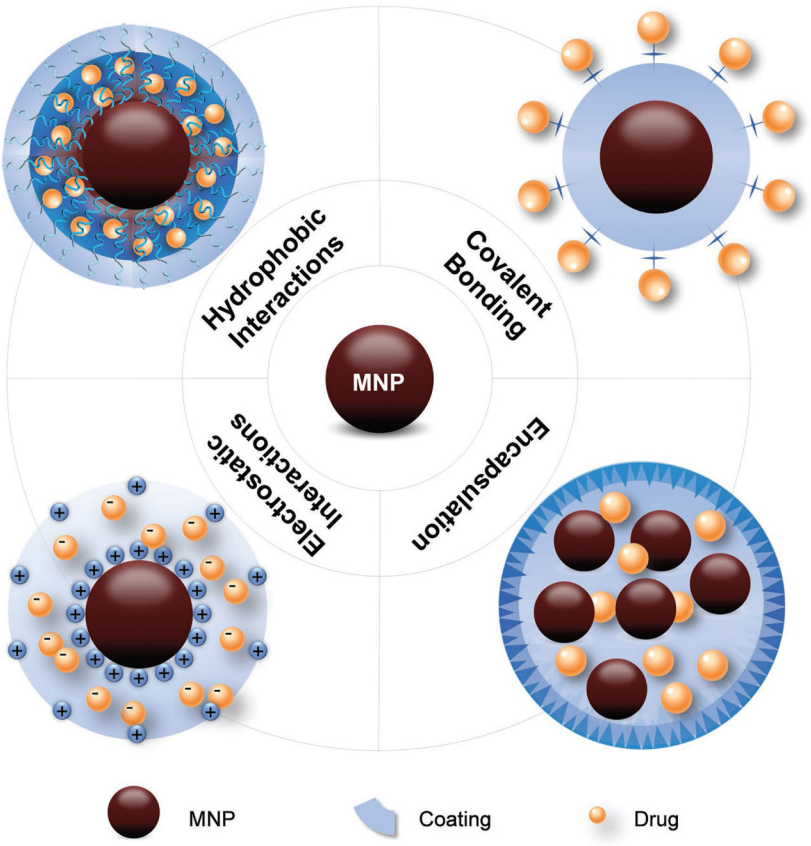

Figure 2.
Illustration of the methods used for loading drugs into MNP nanocarriers, including loading through hydrophobic interactions, electrostatic interactions, covalent bonding and direct encapsulation.

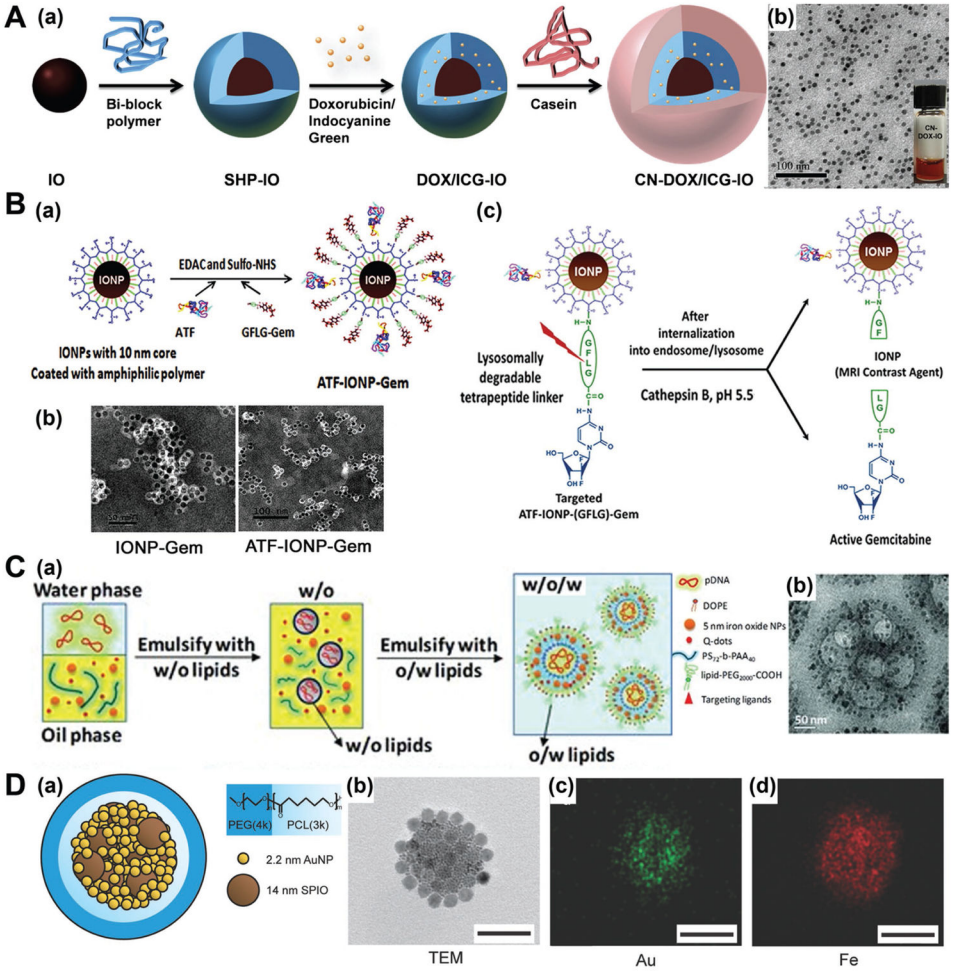

Figure 3.

MNP carriers developed with different drug loading methods. A) Loading through hydrophobic interactions. a) Illustration of drug (Dox) loaded into the hydrophobic layer of a bi-block polymer and wrapped with milk casein protein (CN-DOX-IO); b) Typical TEM images for obtained CN-DOX-IO. Reproduced with permission.[25] Copyright 2015, Elsevier. B) Loading through covalent bonding. a) Diagram of the conjugation of ATF peptides and GFLG-Gem conjugates to IONPs; b) Typical TEM images for non-targeted IONP-Gem and targeted ATF-IONP-Gem with negative staining; c) Schematic diagram of gemcitabine release from ATF-IONP-Gem by enzyme cleavage. Reproduced with permission.[31] Copyright 2014, American Chemical Society. C) Loading through electrostatic interactions. a) Schematic illustration for preparing lipo-polymersome (LPP) nanocarriers with three-compartment structures: 1) a cationic lipids/pDNA core, 2) an IO nanoparticles–polymer composite interlayer, and 3) a relatively neutral lipids shell; b) Typical TEM images of as-prepared LLP nanocarriers. Reproduced with permission.[35] D) Loading by direct encapsulation. a) Schematic of gold- and IONP-loaded polymeric micelles (GSMs). Gold and IONP are self-assembled into the hydrophobic core of micelles, stabilized with the amphiphilic di-block co-polymer PEG-b-PCL; b) TEM image of a single

GSM. (all scale bars = 100 nm); c–d) Energy dispersive X-ray spectroscopy analysis on GSM with Au and Fe signals, respectively. Reproduced with permission.[46]

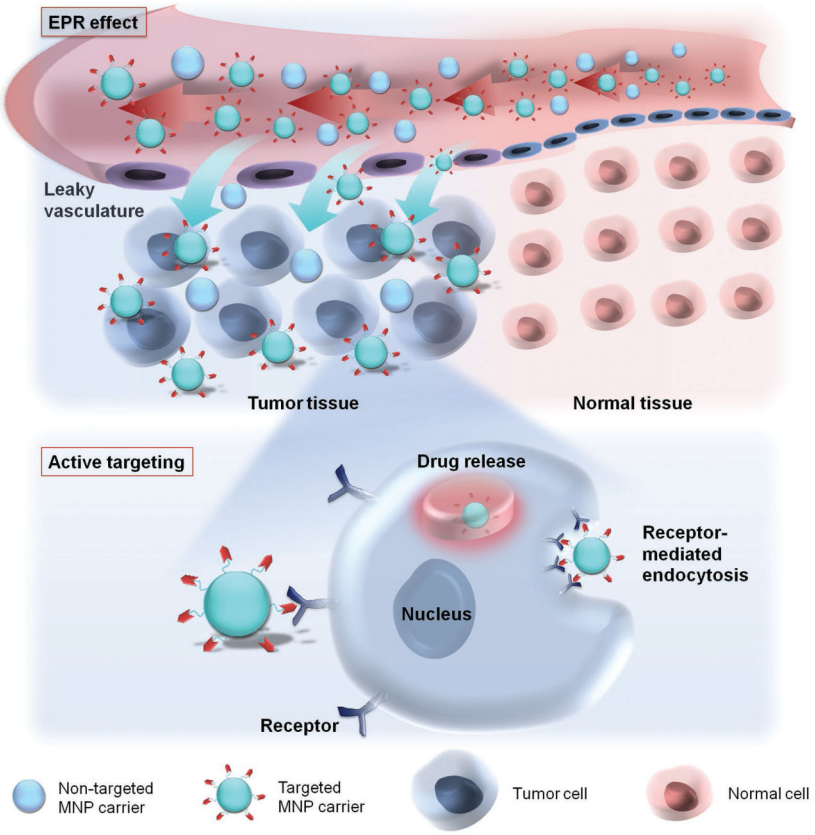

Figure 4.

Illustration of the mechanism of MNP-based drug delivery systems. Taking tumor as an example, MNP-based drug carriers may reach the tumor tissue via the EPR effect due to leaky vasculature, and facilitate active targeting to tumor cells through the conjugated targeting ligands interacting with cellular receptors.

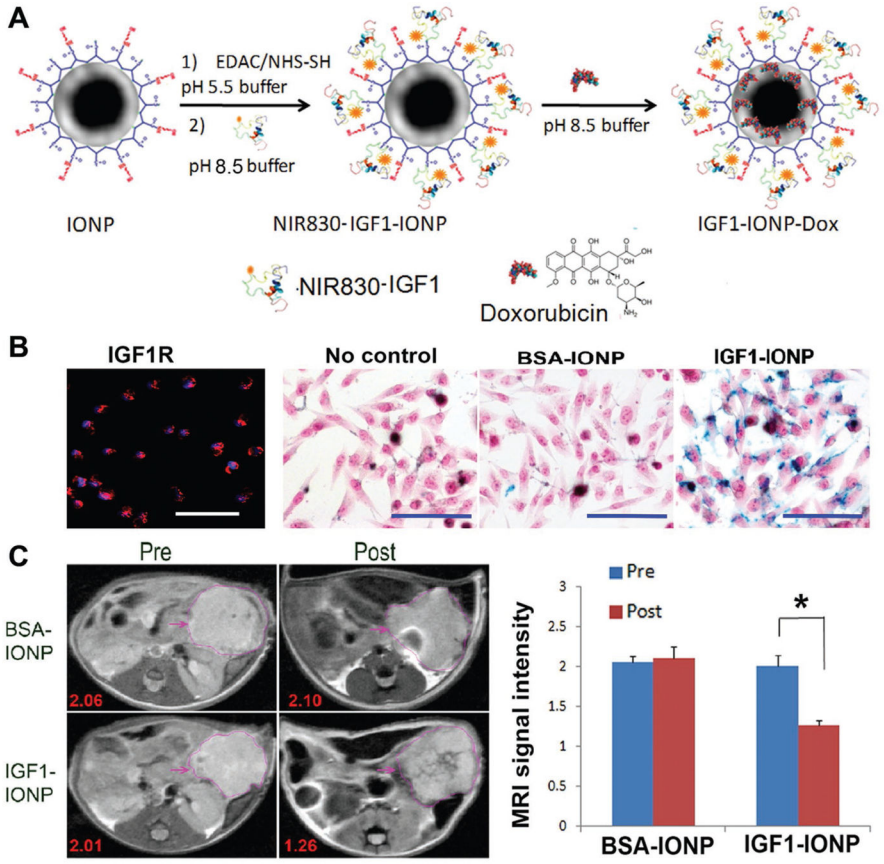

Figure 5.

Targeted MNP carriers for pancreatic cancer treatment. A) Schematic illustration for conjugation of NIR830-IGF1 to amphiphilic polymer-coated IONPs and encapsulation of Dox to MNPs. B) The level of IGF1R in MIAPaCa-2 cells was examined by immunofluorescence labeling using an anti-IGF1R antibody (red), and Prussian blue staining of cells incubated with IONPs, BSA-IONPs, and IGF1-IONPs at 20 μg/mL of iron equivalent dose for 4 h. Scale bars are 100 um. C) Pre and post 24 h T2-weighted MR images. Numbers shown are relative mean MRI signal intensities of the entire tumor. Bar figure shows quantification of MRI signals in the tumors prior to and 24 h after administration of different IONPs. *$p < 0.0001$. Pink arrows indicate the location of pancreatic PDX-tumor lesions. Reproduced with permission.[22] Copyright 2015, American Chemical Society.

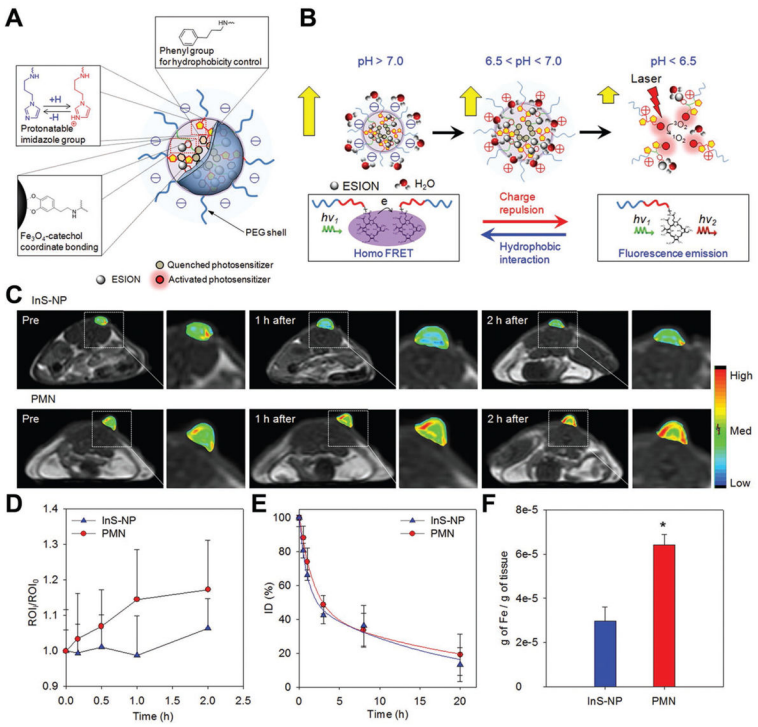

Figure 6.

Enhancing therapeutic effect by tuning the size and charge of MNP carriers through pH-sensitive polymer coating. A) Schematic representation of pH-sensitive magnetic nanogrenades (PMNs) composed of pH-responsive coating, photo-sensitizer and extremely small 3 nm IONPs (ESIONs). B) pH-dependent structural transformation and related magnetic/photoactivity change in PMNs. C) In vivo T_1-weighted MR images and color-mapped images of tumor sites before and 1 or 2 h after intravenous injection of PMNs or pH-insensitive nanoparticle assemblies (InS-NPs) into nude mice bearing HCT116 tumors. D) Plot of signal intensity enhancement (ROI) versus time after injection of PMNs and InS-NPs. E) Blood circulation data (plasma iron concentration vs time) for PMNs and InS-NPs in nude mice (n = 3). F) Inductively coupled plasma atomic emission spectroscopy (ICP-AES) analysis of tumor tissue shows >2-fold increase of PMNs than InS-NPs in HCT116 tumors at 12 h after intravenous injection. Reproduced with permission.[106] Copyright 2014, American Chemical Society.

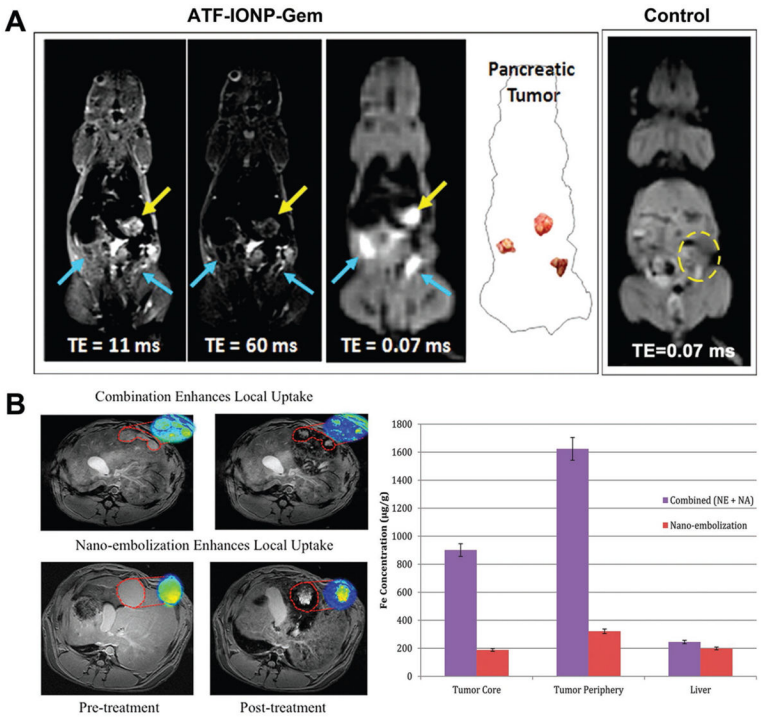

Figure 7.

Visualizing drug delivery in vivo with MNP carriers in an orthotopic human pancreatic cancer xenograft model. A) Comparison of short TE (TE = 11 ms) and long TE T_2-weighted spin echo (TE = 60 ms) and ultrashort TE (TE = 0.07 ms) MR images from a mouse treated with ATF-IONP-Gem. Both primary (pointed out by yellow arrows) and secondary (pointed out by blue arrows) were visualized obviously by using the UTE imaging. Reproduced with permission.[31] Copyright 2013, American Chemical Society. B) Combination nanoablation and nanoembolization versus nanoembolization alone in VX2 rabbit liver cancer model on 7T MRI. Representative axial T_2*W GRE images (TE: 11.9 ms) with corresponding R_2* parametric maps from the same animal. Combination therapy resulted in significant signal change within tumor core and periphery, as depicted in red. Right panel is biodistribution of DOX-SPIOs in tumor and liver tissue following combination therapy (nanoembolization followed by nanoablation) in VX2 rabbit model. ($p < 0.05$). Reproduced with permission.[128] Copyright 2013, American Chemical Society.

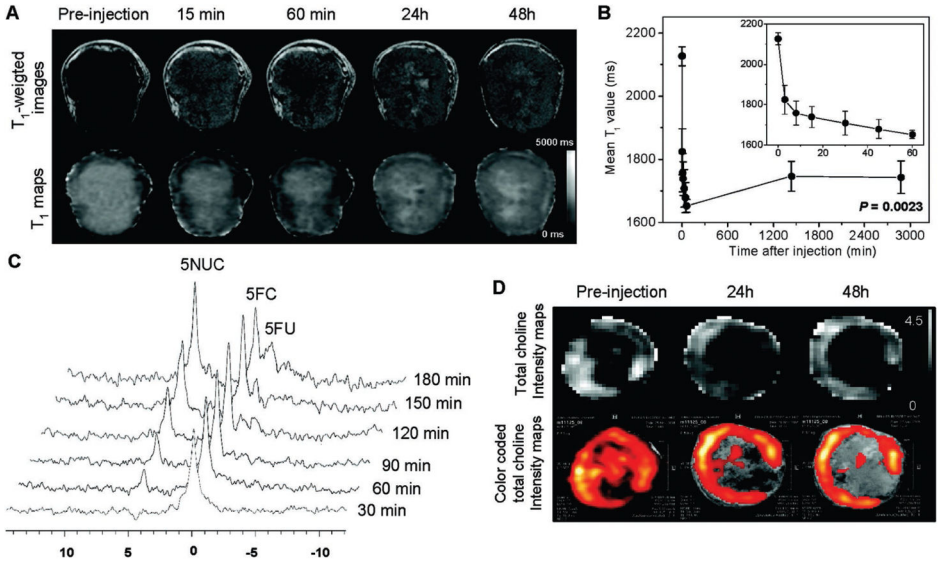

Figure 8.

Monitoring drug delivery with MNP carriers, composed of a nanoplex of PEI/siRNA-chk/PLL-DOTA-Gd/Cy5.5/bCD-111, in a breast cancer xenograft model. A) Representative in vivo T_1-weighted MR images and quantitative T_1 maps of a tumor pre- and post-injection of MNP carriers, showing the distribution of MNP carriers in periphery area of the tumor at 60 min after injection, and in the central region of the tumor after 24 h and 48 h. B) Time-dependent mean T_1 values of tumors (n = 4) pre- and post-injection of nanoplex; a significant decrease of T_1 ($P < 0.0023$) was observed up to 48 h. C) In vivo ^{19}F MRS demonstrated efficient conversion of prodrug 5-FC to 5-FU and its metabolites F-Nucl by nanoplex localized in the tumor. 5-FC was injected at 24 h after nanoplex injection. D) Representative in vivo tCho maps and color-coded tCho intensity maps overlaid on corresponding T_1-weighted images of a tumor before and at 24 and 48 h after nanoplex injection, displaying spatial siRNA-mediated downregulation of Chk-α. Reproduced with permission.[130] Copyright 2010, American Chemical Society.

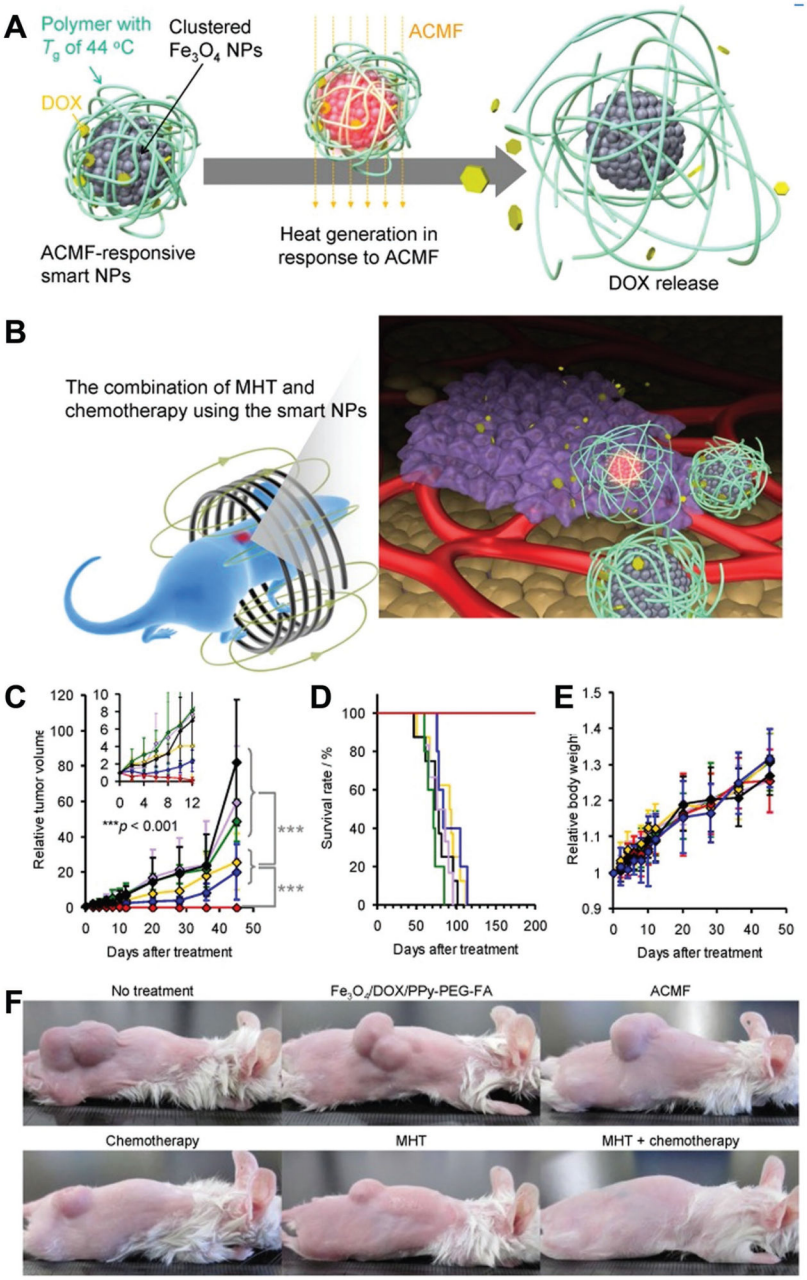

Figure 9.

Combination chemotherapy and hyperthermia with MNP carriers. A) Illustration of MNP carriers that produce heat in response to AMF and sequentially release Dox. B) Illustration of cancer treatment with the combination of magnetic hyperthermia and chemotherapy using the smart NPs. Change of C) tumor volume, D) survival rate, and E) body weight: non-treated mice (black), mice treated with chemotherapy (yellow), mice exposed to AMF (green), mice injected with Fe_3O_4/Dox/PPy-PEG-FA NPs intratumorally (purple), mice treated with magnetic hyperthermia (blue), and mice treated with the combination of magnetic hyperthermia and chemotherapy (red). F) Photographs of non-treated mice, mice

treated with chemotherapy, mice exposed to AMF, mice injected with Fe3O4/Dox/PPy-PEG-FA NPs intratumorally, mice treated with magnetic hyperthermia, and mice treated with the combination of magnetic hyperthermia and chemotherapy 45 days after treatment. Reproduced with permission.[28] Copyright 2015, Ivyspring International Publisher.

Table 1

ed by MNPs with different loading and release methods.

Therapeutics	MNP	Coating Materials	Loading Method	Release Method	Targeting Ligands	Ref.
Doxorubicin	IONP	PMO, PEG, casein, mPEG-poly(L-asparagine), PNIPAM-b-PEI, PAA dendrimer, liposome	hydrophobic interaction, electrostatic interaction, direct encapsulation, covalent bonding	pH- and enzyme-responsive, radio frequency, focused ultrasound	IGF1, PMSA, RGD, magnet	[22,25,28, 107,128,145]
Doxorubicin	liposome-Gadoteridol	liposome	hydrophobic interaction	ultrasound	na	[129]
gemcitabine	IONP	PMO, BSA	covalent bonding, direct encapsulation	pH- and enzyme-responsive	ATF, EGFR mAb C225, magnet	[31,119]
paclitaxel	IONP	PEGylated PAA, TPA-PEP, folate-PEOz-PLA	covalent bonding, hydrophobic interaction	pH	folate	[24,29b]
Hydroxy-camptothecin	IONP	PEGylated chitosan	hydrophobic interaction	radio frequency	na	[28]
Epirubicin	IONP	PMO	covalent bonding	pH-sensitive	magnet	[37]
EGFRvIIIAb	IONP	PMO	covalent bonding	na	EGFRvIIIAb	[124]
siBIRC5	IONP	cross-linked dextran	covalent bonding	na	peptides (EPPT)	[123a]
siRNA-chk, bcd-111	Gd-DOTA	PEI/siRNA-chk/PLL-DOTA-Gd/Cy5.5/bCD-111	electrostatic interaction, covalent bonding	na	na	[130]
DNA	IONP	PEI-, PEG-chitosan	electrostatic interaction	endosomal release	na	[42]
Stem Cell	Magnetosomes	na	Gene transfection	na	na	[125]
Stem cell	IONP	silica	cellular internalization	na	na	[135]
MDMs with HSV1716	IONP	na	cellular internalization	na	magnetic field gradient	[121]
AuNPs	IONP	PEG-b-PCL	direct encapsulation	radiation	na	[46]
Mitomycin C	UCNPs (NaYF4:Yb/Er/Tm/Gd)	mesoporous silica	direct encapsulation	radiation	TAT	[138]
captopril stabilized-Au nanoclusters	UCNPs doped with Gd3+	mesoporous silica, PAAM, PEG	electrostatic interaction	laser		[139]
Au NPs	IONP	Silica, Dopamine, PEG	direct encapsulation, electrostatic interaction	laser	magnet	[120,144]
Dox, Co_9Se_8, FeS	Co_9Se_8, FeS	PAA, PEGylated OAePAA-PAH	electrostatic interaction	laser		[131,139]
GO, Fe_2C_5	IONP, Fe_2C_5	DSPE-PEG-NH_2	precipitation	laser	affinity ZHER2:342	[99,140]
pyrrole, IR825, chlorin e6	Gd-PEG-PPy NPs, Gd III-chlorin e6	PEG-Ppy, PEGylated C18PMH	covalent bonding, hydrophobic interaction	laser	na	[132,133]
Heparin-pheophorbide-A	IONP	APTES	covalent bonding	laser	na	[143]

Table 2

Methods for Introducing Targeting Ligands on MNP Surface.

	Active group on MNP	Active group on ligand	Linker	Ligand type	In vivo In vivo application	Ref
Direct Conjugation	Amine	Carboxyl		Aptamer, protein, small molecule	prostate, breast, pancreatic cancer	[82–96]
		Anhydride		Small molecule	pancreatic cancer	[96]
	Carboxyl	Amine		Protein, Peptide, aptamer	breast, prostate, pancreatic cancer	[22,31–97]
	Aldehyde	Amine		Protein	rectal and mammary carcinoma	[84–100]
	Amine	Thiol (thiolation through amine)	SIA to activate amine MBNHS to activate amine	Small molecule	gliomas, pancreatic cancer	[101–103]
Linker Conjugation		Alkyne	synthetic linker	peptide	breast cancer	[104]
		Amine	Sulfo-LC-SPDP to activate both MNP and ligand	peptide	breast cancer	[69]
	Hydroxyl	Carboxyl	EDBE to activate hydroxyl	protein	breast cancer	[68]
	Thiol	Amine	sulfo-SMCC to activate amine	protein	breast cancer	[105]